AD-A103 279 SACLANT ASW RESEARCH CENTRE LA SPEZIA (ITALY) F/G 20/4
A REVIEW OF ONE-DIMENSIONAL OCEANIC MIXED-LAYER MODELS,(U)
MAY 81 J MOEN
UNCLASSIFIED SACLANTCEN-SR-47 NL

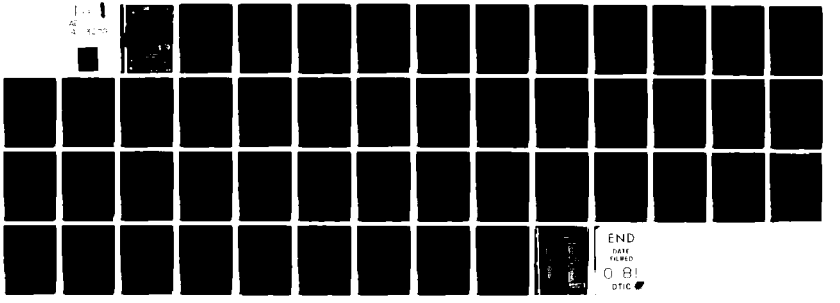

LEVEL II

SACLANTCEN Report SR-47

SACLANT ASW
RESEARCH CENTRE
REPORT

AD A103279

A REVIEW OF ONE-DIMENSIONAL OCEANIC MIXED-LAYER MODELS

by

JON MOEN

DTIC
ELECTE
AUG 25 1981
S D
A

1 MAY 1981

This document has been approved for public release and sale; its distribution is unlimited.

NORTH
ATLANTIC
TREATY
ORGANIZATION

LA SPEZIA, ITALY

DTIC FILE COPY

81 8 25 078

14 SACLANTCEN [redacted]T-SR-47

NORTH ATLANTIC TREATY ORGANIZATION

SACLANT ASW Research Centre
Viale San Bartolomeo 400, I-19026 San Bartolomeo (SP), Italy

tel: national 0187 560940
international + 39 187 560940

telex: 271148 SACENT I

A REVIEW OF ONE-DIMENSIONAL OCEANIC MIXED-LAYER MODELS

by

Jon Moen

1 May 1981

12 15p

This report has been prepared as part as Project 04.

APPROVED FOR DISTRIBUTION

B.W. LYTHALL
Director

TABLE OF CONTENTS

A REVIEW OF ONE-DIMENSIONAL OCEANIC MIXED-LAYER MODELS

by

Jon Moen

ABSTRACT

An overview of the available one-dimensional mixed-layer models is presented. A number of specific models, developed from a common set of basic equations, are discussed and inter-compared. While many of the models report satisfactory agreement with observational data, they depend strongly on the choice of empirical parameters. It is pointed out that no particular mechanism has emerged to fully explain observations of 'slab-like' (vertically uniform) flow in the mixed layer and so, despite the use of slab-flow in simplifying bulk model equations, its cause has not been properly recognized. That some extra mechanism is required can be seen in the results of the differential models, which do not predict slab-like flow unless the wind subsides. A complete bibliography is provided.

INTRODUCTION

Over the past decade a number of models have been put forward in an attempt to explain the important time-dependent features of the oceanic mixed layer. They have met with varying degrees of success when tested against field observations and laboratory experiments.

An outline of the various general approaches to one-dimensional, upper-ocean models has been given by Niiler & Kraus *[1]*. A comprehensive treatment of mixed-layer forming mechanisms was presented there and these were unified into a generalized bulk (vertically integrated) model. A similar, although less descriptive, generalized bulk model was developed by Kim *[2]*. Another very comprehensive review treating the historical development by mechanisms rather than by a series of over-lapping models has recently been presented by Zilitinkevich, Chalikov, & Resnyansky *[3]*. Such approaches will not be followed in this review; instead, various mechanisms and approximations will be discussed as they occur in relation to each particular model. Comparison between models will be made easier by use of a consistent notation throughout. Of the many models only ten have been singled out for discussion, with the intention that this choice should provide a clear overview of the development and present state of mixed-layer modelling. This does not mean to imply, however, that models excluded from this review are unimportant.

The models to be reviewed fall fundamentally into two categories: those that specifically include the effect of the earth's rotation, and hence inertial oscillations, and those that do not. The latter begin with the model of Kraus & Turner *[4]* and assume that layer-deepening occurs primarily through downward turbulent transport of the turbulent energy imparted to the surface by the wind. The turbulent energy available for mixing in such models is usually parameterized as a constant fraction of the downward wind-energy flux at 10 m. The former category begin with the model due to *Pollard, Rhines, & Thompson [5]*, who proposed that the major effect of the wind acting on the sea surface was to introduce inertial oscillations into the mixed layer. The effect of this would be to increase the velocity shear at the mixed-layer base, thus reducing the Richardson number there and causing the instabilities and turbulent entrainment necessary for layer deepening. Such models assume a 'slab-like' motion of the mixed layer with mean velocity shear only within thin upper and lower boundary layers.

Another model due to Niiler *[6]* combines both the inertial oscillation and parameterized wind-stress approaches. This argues that since mixed layers continue to deepen after the initial one-half pendulum-day period (in which all of the deepening is predicted to occur by the Pollard, Rhines & Thompson model *[5]*) a continuous and slow erosion process from surface, wind-generated turbulence must also be present.

A later model by Garwood *[7]*, although including the effects of rotation, represents a departure from the earlier models. Rather than assuming a slab-flow approximation, a more rigorous treatment is carried out in which

the bulk flow is taken to be the vertically-averaged flow. Shear production of turbulent kinetic energy within the mixed layer can then be explicitly recognized. The source of entrainment energy consists entirely of surface production and any shear production within the entrainment zone is considered to be negligible. The Richardson number is therefore not the critical parameter determining entrainment, and the important effect of rotation is not in reducing the Richardson number as in the Pollard, Rhines & Thompson model *[5]*, but rather in influencing the dissipation time scale.

All of the models to be described employ the same basic hydrodynamic and thermodynamic equations, which, when integrated vertically, have simplified bulk forms. In models employing the slab-flow approximation the bulk-energy equations become yet further simplified through use of the bulk-momentum equation in parameterizing energy production at the lower entrainment interface. In fact, the magnitude of the production term, and hence the model performance, depends strongly on the slab-flow approximation. It will become clear in the course of the review, however, that although the observation of slab-like motion is recognized by stipulation in bulk models, possible mechanisms causing the slab have not been proposed nor accounted for in any way in energy-balance equations.

1 THE BASIC EQUATIONS

We now proceed by writing down the mixed-layer equations that will form a basis for the description of all the models contained in this review. Derivations, when required, are presented in Appendix A.

For some of the models we do not need to specify the mean velocity profile within the mixed layer. For others we consider a mixed layer, depicted schematically in Fig. 1, to be composed of three sublayers: a thin upper shear layer of thickness d induced by the wind blowing over the sea surface, a thick middle layer of thickness h-d containing no shear, and a thin lower shear layer of thickness δ caused by the entrainment friction of the mixed layer sliding over the stratified fluid below. In all the bulk models temperature and salinity are taken to be constant with depth throughout the upper and middle layers and all field variables are taken to be horizontally homogeneous. The stratified water underlying the mixed layer is taken to be at rest below some level z = -H, where $H \gg h+\delta$. We shall not be concerned with the effects of internal waves nor, apart from Denman's model (Ch. 3), of horizontal advection.

The vertically integrated mean and turbulent mechanical energy equations are written as

$$\frac{\partial}{\partial t}(KE_m) + \bar{\rho}_o \underline{\bar{u}}_o \cdot (\overline{\underline{u}'w'})_o - \int_{-H}^{o} \bar{\rho}_o (\overline{\underline{u}'w'}) \cdot \frac{\partial \underline{\bar{u}}}{\partial z}\, dz = 0 \qquad \text{(Eq. 1)}$$

and

$$\frac{\partial}{\partial t}(\overline{KE_t}) + \int_{-H}^{o} \bar{\rho}_o (\overline{\underline{u}'w'}) \cdot \frac{\partial \underline{\bar{u}}}{\partial z}\, dz + [\overline{w'p'} + \overline{w'KE_t'}]_o + g \int_{-H}^{o} \overline{w'\rho'}\, dz + \varepsilon = 0, \qquad \text{(Eq. 2)}$$

respectively, where

$$KE_m = \int_{-H}^{o} \bar{\rho}(\bar{u}_1^2 + \bar{u}_2^2) / 2\, dz$$

$$KE_t' = \int_{-H}^{o} \rho(u_1'^2 + u_2'^2 + u_3'^2) / 2\, dz ,$$

and ε is the total rate of dissipation of turbulent energy within the water column. The second term in Eq. 1 represents the input of mechanical energy supplied by the wind acting at the sea surface and the third term represents the transfer of energy from the mean to the turbulent flow by action of the

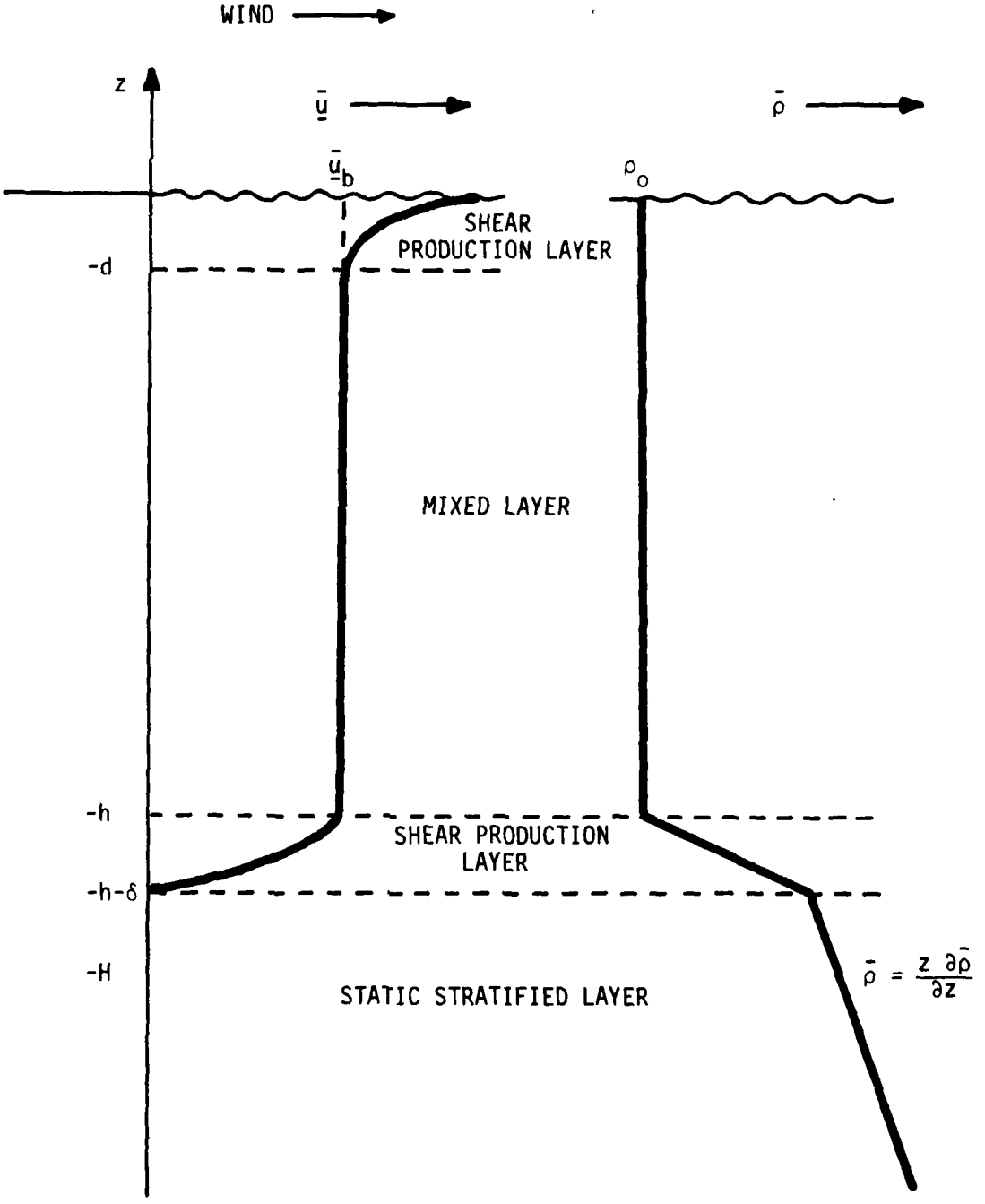
WIND
z
$\bar{u}$
$\bar{\rho}$
$\bar{u}_b$
ρ_o
SHEAR
PRODUCTION LAYER
-d
MIXED LAYER
-h
SHEAR PRODUCTION
LAYER
-h-δ
-H
STATIC STRATIFIED LAYER
$\bar{\rho} = \frac{z\ \partial\bar{\rho}}{\partial z}$

Fig. 1

Reynolds' stresses ($\overline{u'w'}$) on the mean shear. The contribution to the latter is assumed, in most models, to be mainly from the upper and lower shear boundary layers. The third term of Eq. 2 represents the rate of working by the normal pressure fluctuations in the wind field flowing over the waves together with a surface energy flux due to breaking waves. The magnitude of this term is largely unknown and its parameterization in the various models ought, therefore, to be treated with some caution. The fourth term of Eq. 2 represents the total vertical mass flux (or negative buoyancy flux) per unit area within the layer and, in the absence of any solar penetration, is equal to the rate of change in gravitational potential energy PE within the layer, given by

$$\frac{\partial}{\partial t}(\overline{PE}) - g\int_{-H}^{0}(\overline{w'\rho'})dz - \frac{g\alpha I_o}{\gamma c} = 0, \qquad \text{(Eq. 3)}$$

where I_o is the surface value of the penetrating component of solar radiation, $I = I_o e^{\gamma z}$, α is the thermal expansion coefficient, and c is the specific heat of sea water at constant pressure. Equation 3 was obtained by multiplication of the local mass conservation equation

$$\frac{\partial\overline{\rho}}{\partial t} + \frac{\partial}{\partial z}(\overline{w'\rho'} + \frac{\alpha}{c} I) = 0 \qquad \text{(Eq. 4)}$$

by the vertical coordinate before integration. Equation 4 represents the combined conservation equations for heat and salt and could, by applying the transformation

$$\cdot \rightarrow -g\frac{(\rho-\rho_r)}{\rho_r} = b,$$

be called a buoyancy conservation equation. We prefer to work with the density variable, however, because then it can more easily be replaced by $\rho_r\alpha T$ for comparisons with models that neglect salinity effects on density. Integration of Eq. 4 yields the bulk mass conservation equation

$$h\frac{\partial\overline{\rho}_o}{\partial t} + (\overline{w'\rho'})_o - (\overline{w'\rho'})_{-h} + \frac{\alpha}{c} I_o(1-e^{-\gamma h}) = 0. \qquad \text{(Eq. 5)}$$

Another expression for the potential energy is obtained by considering the observed geometry of a deepening mixed layer, which gives

$$\frac{\partial}{\partial t}\overline{PE} + \mathcal{H}gh(\overline{\rho}_o - \overline{\rho}_{-h-\delta})\frac{\partial h}{\partial t} + g\frac{h^2}{2}\frac{\partial\overline{\rho}_o}{\partial t} - g\frac{\alpha}{c} I_o e^{-\gamma h}(h+\gamma^{-1}) = 0, \qquad \text{(Eq. 6)}$$

where $\mathcal{H}$ is the unit Heaviside function, having the value unity when $\frac{\partial h}{\partial t}$ is positive and zero otherwise. The fourth term of Eq. 6 arises due to the

density changes below the mixed layer and is derived from the term

$$-\int_{-\infty}^{-h} gz \frac{\partial \bar{\rho}}{\partial t} dz$$

together with use of Eq. 4 . This term, however, is normally neglected for large values of h.

It can be shown (see App. A.) that the bottom boundary condition for the mass flux is

$$-(\overline{w'\rho'})_{-h} = \mathcal{K}(\rho_o - \rho_{-h-\delta}) \frac{\partial h}{\partial t} . \qquad \text{(Eq. 7)}$$

Using this condition, Eqs. 5 and 6 combine to give another useful form

$$\frac{\partial}{\partial t} \overline{PE} + \mathcal{K} g \frac{h}{2} (\rho_o - \rho_{-h-\delta}) \frac{\partial h}{\partial t} - [g \frac{h}{2} (\overline{w'\rho'})_o + g \frac{\alpha h}{2c} I_o]$$

$$- g \frac{\alpha I_o}{c} e^{-\gamma h} (\frac{h}{2} + \gamma^{-1}) = 0 \qquad \text{(Eq. 8)}$$

for the changing potential energy of the layer.

Finally, we write the bulk momentum equation for the layer as

$$\frac{\partial \bar{M}}{\partial t} + \underline{f} \times \bar{M} - \bar{\tau}_o = 0, \qquad \text{(Eq. 9)}$$

where $\bar{M}$ is the total mean momentum of the layer, given by

$$\bar{M} = \rho_o \int_{-H}^{o} \bar{u} \, dz.$$

If a slab-like motion is assumed, Eq. 9 can be written in the form

$$h \frac{\partial}{\partial t} \bar{u}_b + h(\underline{f} \times \bar{u}_b) + \bar{y}_b \frac{\partial h}{\partial t} - \frac{\bar{\tau}_o}{\rho_o} = 0. \qquad \text{(Eq. 10)}$$

Here the second term represents the effect of the earth's rotation and the third the bottom boundary condition

$$(\overline{u'w'})_{-h} = -\bar{u}_b \frac{\partial h}{\partial t} , \qquad \text{(Eq. 11)}$$

which simply describes the downward momentum flux across the lower boundary as the layer deepens.

2 KRAUS & TURNER MODEL (1967)

We begin with the theory due to Kraus & Turner *[4]*, since it is effectively the forerunner to a host of similar theories to follow it. The only important addition to their theory was to come later when Pollard, Rhines & Thompson *[5]* included the effects of inertial oscillations in mixed-layer deepening, but this will be dealt with separately later.

By substitution of Eq. 3 into Eq. 2 to eliminate the total mass-flux term, and addition of the mean Kinetic energy equation (Eq. 1) we obtain the mechanical energy balance

$$\left\{ \frac{\partial}{\partial t} \overline{PE} - \frac{g\alpha}{\gamma c} I_o \right\} + \frac{\partial}{\partial t} (KE_m + \overline{KE}_t) + \left\{ \left[\overline{w'p'} + \overline{w'KE'_t} \right]_o - \underline{\bar{u}}_o \cdot \underline{\bar{\tau}}_o \right\} + \varepsilon = 0, \qquad \text{(Eq. 12)}$$

which was written down but not derived by Kraus & Turner in the form

$$w^* + G^* - D^* = 0. \qquad \text{(Eq. 13)}$$

In Eq. 13 w^* corresponds to the first term of Eq. 12 and represents the change in potential energy due to mechanical stirring or free convection. We see that it is the rate of change of total potential energy, minus that portion, $\frac{g\alpha}{\gamma c} I$, due to the penetrating component of solar radiation. G^* is the kinetic energy input from the wind, some of which will be dissipated by the term D^*. Since, from Eq. 13, $D^* = -\varepsilon$ we deduce that

$$G^* = \frac{\partial}{\partial t}(KE_m + \overline{KE}_t) + \left[\overline{w'p'} + \overline{w'KE'_t} \right]_o - \underline{\bar{u}} \cdot \underline{\bar{\tau}}_o \qquad \text{(Eq. 14)}$$

Which, if any, of these terms Kraus & Turner intended to ignore is not known, but taking into account that G^* is set equal to a constant in their treatment it is reasonable to assume that those contributions to Eq. 14 that could vary with the inertial oscillations were implicitly neglected. Also, on the time scales considered, the turbulent energy $\overline{KE}_t$ can be presumed invariant. We will not attempt to separate out these effects from Eq. 14 since it would be presumptuous and, in any case, this sort of approach has been carried out by others (e.g., Niiler, *[6]*) using slab models and so will be discussed later.

We note that in Kraus & Turner's application of their model to their laboratory results *[9]* no mean flow was generated and so the neglect of inertial oscillations from G^*, though inadvertent, was perfectly in order.

Elimination of the potential energy term between Eqs. 12 and 6, and neglecting the kinetic energy term, yields

$$g\frac{h^2}{2}\frac{\partial\bar{\rho}_o}{\partial t} + \mathcal{K}gh(\bar{\rho}_o - \bar{\rho}_{-h-\delta})\frac{\partial h}{\partial t}$$

$$= G^* - D^* - \frac{g\alpha}{\gamma c} I_o - g\frac{\alpha}{c} I_o e^{-\gamma h}(h+\gamma^{-1}), \qquad \text{(Eq. 15)}$$

which is equivalent to Kraus & Turner's equation 10 if the term in $e^{-\gamma h}$ is ignored.

The model then consists of bulk equations describing two regimes. One regime assumes mixed-layer deepening, in which case the function $\mathcal{K} = 1$ and the energy balance (Eq. 15) is integrated in time to give

$$\left[g\frac{h^2}{2}\bar{\rho}_o\right]_{t=t_2}^{t} - g\int_{h(t=t_2)}^{h(t)} \bar{\rho}_{-h-\delta}\, h\, dh = \int_{t=t_2}^{t} \left(G^* - D^* - g\frac{\alpha I_o}{\gamma c}\right) dt, \qquad \text{(Eq. 16)}$$

and the mass conservation equation (Eq. 5), modified by the entrainment boundary condition (Eq. 7), is integrated to give

$$[h\bar{\rho}_o]_{t=t_2}^{t} - \int_{h(t=t_2)}^{h(t)} \bar{\rho}_{-h-\delta}\, dh = \int_{t=t_2}^{t} \left[-(\overline{w'\rho'})_o - \frac{\alpha I_o}{c}\right] dt\ . \qquad \text{(Eq. 17)}$$

These two equations require a foreknowledge of the initial values of $\bar{\rho}_o(t_2)$ and $h(t_2)$ together with the profile of $\bar{\rho}$ below $h(t_2)$. The integrands on the right of Eqs. 16 and 17 are specified functions of time.

In the other regime the mixed layer is not deepening, in which case $\mathcal{K} = 0$ and Eqs. 5 and 15 give

$$h = \frac{2\left(G^* - D^* - \frac{g\alpha I_o}{\gamma c}\right)}{g\left[-(\overline{w'\rho'})_o - \frac{\alpha}{c} I_o\right]} \qquad \text{(Eq. 18)}$$

and

$$[\bar{\rho}_o]_{t=t_1}^{t} = \int_{t=t_1}^{t} \left[-(\overline{w'\rho'})_o - \frac{\alpha I_o}{c}\right] dt\ . \qquad \text{(Eq. 19)}$$

Kraus & Turner investigate a simple case where the dissipation D* is set to zero, the penetrating solar radiation ignored by setting $\gamma = \infty$, and a constant rate of working G* by the wind is assumed. The surface-heating term

$-(\overline{w'T'})_o - \frac{I_o}{c\rho_r}$ is then given a saw-tooth distribution in time and applied

to Eqs. 18, 19, 16 and 17, in that order. These then reduce to a simple set of algebraic equations in $\bar{\rho}_o$ and h. Note that we have switched to the heating term here by replacing ρ' by $\rho_r \alpha T'$ in the density flux term of Eqs. 18 and 19.

The saw-tooth heating function chosen is of interest both because it can be compared directly with earlier laboratory experiments by Turner & Kraus *[9]* and because it simulates the daily and seasonal heating cycles quite well. Kraus & Turner report, for example, that a sinusoidal heating function that they tried gave very similar results.

The model predicts the following general features of seasonal variations within the mixed layer:

1) The interface rises during the heating cycle, with a minimum depth at the time of maximum heating.

2) The time of maximum temperature lags behind the time of maximum heating and minimum depth but precedes the time of zero cooling.

3) The temperature of the layer is proportional to the square of the maximum rate of heating and increases linearly with the period over which heating occurs. It is inversely proportional to the rate of kinetic energy input by the wind.

4) The depth of the layer is directly proportional to the mechanical stirring rate and inversely proportional to the heating.

Comparisons with observations at Ocean Weather Station (OWS) PAPA *[10]* in the northeastern Pacific is made by first setting

$$G^* = |\bar{\tau}_o|\, u_w^* = \rho_a\, u_a^{*3} \sqrt{\frac{\rho_a}{\rho_o}} \ ,$$

where u_w^* is the water-friction velocity and u_a^* the air-friction velocity calculated from the drag coefficient and wind velocities at 10 m using the relation

$$u_a^* = C_{10}\, U_{10}^2 \ .$$

Choosing the average values 1.7×10^{-3}, 8 m/s, and 400 cal/cm^2/day for C_{10}, U_{10} and the downward surface-heat transfer respectively, gave the results h_{min} = 26 m and T_{max} = 9°C, both lying within the observed ranges. Kraus & Turner note, however, that their model predictions lie well outside the observed ranges if penetrative radiation and hence convective mixing are included. They argued, though, that dissipation should also be included and predictions might then be improved.

3 DENMAN MODEL (1973)

An approach similar to that of Kraus & Turner but using somewhat different parameterization and allowing for a variable wind stress was adopted by Denman *[8]*. The purpose and design of the model was to obtain quantitative results over a time scale of several days rather than months (as in the Kraus & Turner model), to allow for a meteorological input varying in time and to include insolation and mean upwelling effects below the lower interface.

The mean-flow kinetic energy balance is not in itself considered, but instead, and in common with other treatments to follow, the starting point is the turbulent kinetic energy balance. However, this distinction is of little significance, since the mean and turbulent energy equations are not mutually exclusive descriptions of the flow.

Elimination of the potential energy term between Eqs. 3 and 6 yields an expression for the total mass flux within the layer given by the third term of Eq. 20. The turbulent energy balance (Eq. 2) is then written as

$$\frac{\partial}{\partial t}(\overline{KE}_t) + \left\{ \int_{-H}^{0} \bar{\rho}_o (\overline{\underline{u}'w'}) \cdot \frac{\partial \bar{\underline{u}}}{\partial z}\, dz + [\overline{w'p'} + \overline{w'KE'_t}]_{z=0} \right\}$$

$$+ \left\{ -\mathcal{H} gh(\bar{\rho}_o - \rho_{-h-\delta}) \frac{\partial h}{\partial t} - g \frac{h^2}{2} \frac{\partial \bar{\rho}_o}{\partial t} - \frac{g\alpha}{c\gamma} I_o \right.$$

$$\left. + \frac{g\alpha}{c} I_o e^{-\gamma h}(h+\gamma^{-1}) \right\} + \varepsilon = 0. \qquad \text{(Eq. 20)}$$

The second term of Eq. 20 is labelled as -G*, the dissipation ε as D*. Substituting for $\frac{\partial \bar{\rho}_o}{\partial t}$ by use of the mass conservation equation (Eq. 5) and boundary condition (Eq. 7), neglecting $\frac{\partial(\overline{KE}_t)}{\partial t}$, and rearranging, gives

$$\mathcal{H}\left(\bar{w} + \frac{dh}{dt}\right) = \frac{1}{gh(\bar{\rho}_o - \bar{\rho}_{-h-\delta})} \left\{ 2\left[-G^* + D^* - \frac{g\alpha}{\gamma c} I_o(1-e^{-\gamma h})\right] \right.$$

$$\left. + gh\left[(\overline{w'\rho'})_o + \frac{g\alpha I_o}{c}(1+e^{-\gamma h})\right] \right\}, \qquad \text{(Eq. 21)}$$

where $\bar{w}$ is a slow upwelling velocity below the well-mixed layer included to allow for large-scale horizontal convergence or divergence. Although, for brevity, $\bar{w}$ was not included in the basic equations, it is clear that these equations must describe deepening or shallowing relative to any mean

vertical motion of the fluid itself. The absolute derivatives in Eqs. 21 and 22 are permitted because the only horizontal inhomogeneity is that giving rise to $\bar{w}$. Since this is assumed to have a very large horizontal scale it can be ignored in the equations.

Next, by substitution for $gh(\bar{\rho}_o - \rho_{-h-\delta}) \frac{\partial h}{\partial t}$, again by use of the mass conservation (Eq. 5), Eq. 20 becomes

$$\frac{d\bar{\rho}_o}{dt} = \frac{2}{gh^2} \left\{ G^* - D^* - gh(\overline{w'\rho'})_o - g\frac{\alpha}{c} I_o(h-\gamma^{-1}) - \frac{g\alpha}{c\gamma} I_o e^{-\gamma h} \right\}. \quad \text{(Eq. 22)}$$

The density profile below the interface is known at any given time but, unlike in the Kraus & Turner model, it is permitted to change in time according to the insolation and upwelling effects described by the mass conservation

$$\frac{\partial\bar{\rho}}{\partial t} + \bar{w}\frac{\partial\bar{\rho}}{\partial z} + \frac{\alpha}{c}\gamma I_o e^{\gamma z} = 0. \quad \text{(Eq. 23)}$$

The density at the descending interface can then be calculated from the relation

$$\frac{d}{dt}\bar{\rho}_{-h-\delta} = \frac{\partial\bar{\rho}}{\partial t}\bigg|_{z=\text{const.}} - \frac{dh}{dt}\frac{\partial\rho}{\partial z}\bigg|_{z=-h-\delta}$$

$$= -(\bar{w} + \frac{dh}{dt})\frac{\partial\bar{\rho}}{\partial z}\bigg|_{-h-\delta} - \frac{\gamma\alpha}{c} I_o e^{\gamma z}, \quad \text{(Eq. 24)}$$

where use of Eq. 23 has been made.

Equations 21, 22 and 23 are then the ordinary differential equations representing Denman's model. The model allowed Denman to explore a variety of wind- and heat-dominated regimes with boundary conditions varying in time. An analytic solution is presented in the simple case of no heat exchanges, no dissipation, no imposed upwelling velocity $\bar{w}$, a constant wind speed, and a linear density profile $L = \frac{\partial\rho}{\partial z}$ below the mixed layer. In this case it is found that the mixed-layer depth is given by

$$h = (\frac{12G^*}{L})^{1/3} t^{1/3}. \quad \text{(Eq. 25)}$$

Equation 25 agrees well with an earlier independent derivation by Kato & Phillips *[11]* and also with their laboratory experiments and those of Moore & Long *[12]*.

Following Turner *[13]*, Denman introduced an empirically determined constant, m, specifying the fraction of the downward wind energy flux at 10 m available for mixing. Equating this fraction to the mixing energy rate gives

$$G^* - D^* = m|\underline{\tau}|U_{10} \ . \qquad \text{(Eq. 26)}$$

Next, using the argument that the stress $|\underline{\tau}|$ above and below a thin molecular surface boundary layer must be equal, and assuming that the mixing energy rate in the water can also be given by

$$u_w^* \ |\underline{\tau}| \ = \ u_a^*(\rho_a/\rho_o)^{\frac{1}{2}} \ |\underline{\tau}|$$

$$= C_{10}^{\frac{1}{2}} \ U_{10}(\rho_a/\rho_o)^{\frac{1}{2}} \ |\underline{\tau}| , \qquad \text{(Eq. 27)}$$

where the water-friction velocity u_w^* has been replaced by $u_a^*(\rho_a/\rho_o)^{\frac{1}{2}}$ and the air-friction velocity u_a^* by $C_{10}^{\frac{1}{2}} \ U_{10}$, Eqs. 26 and 27 show that

$$m = (C_{10} \ \rho_a/\rho_o)^{\frac{1}{2}} \ . \qquad \text{(Eq. 28)}$$

The value of m = 0.0012, estimated from Eq. 28 was used by Kraus & Turner *[4]* and also by Denman *[8]* and Denman & Miyake *[14]* in their model comparisons with observation at OWS PAPA in the northeastern Pacific. The agreement with observation was found to be very good.

As mentioned earlier, m should in fact be an empirically determined constant. Neglecting heat exchanges with the atmosphere and any radiation of energy away from the lower boundary by internal waves, Eqs. 2 and 3 show that the rate of change in the potential energy of the layer is exactly equal to that of the available mixing energy — however parameterized. Since the potential energy change in a water column can be calculated by taking density profiles before and after a storm, and since the downward wind energy flux at 10 m can be integrated over the same period, values of the fraction m can be estimated. Note that for this fraction to be useful in a mixed-layer prediction model it ought to be universal and invariable. We see, however, that the value of 0.0012 used by Denman & Miyaka *[14]* does not agree with that of 0.01 estimated by Turner *[13]* using data collected in the southwestern North Atlantic. Clearly, the fraction of energy transferred from the wind into mixing energy is not a constant and would appear, at least in the two instances cited above, to be a result of different physical processes. If we consider the parameter

$$G^* = -[\overline{w'p'} + \overline{w'KE_t'} \ ]_o - \int_{-H}^{o} \overline{\rho}_o \ \overline{\underline{u}'w'} \ \frac{\partial \overline{\underline{u}}}{\partial z} \, dz \qquad \text{(Eq. 29)}$$

and replace the integral, using the mean kinetic energy equation (Eq. 1) to give

$$G^* = -[\overline{w'p'} + \overline{w'KE_t'}]_o + \overline{\underline{u}}_o \cdot \overline{\underline{\tau}} - \frac{\partial}{\partial t} \ \overline{KE}_m \qquad \text{(Eq. 30)}$$

we see that, apart from the sign, G* is identical to the form (Eq. 14) we earlier attributed to Kraus and Turner *[4]*. However, Denman assumes that the available mixing energy in the layer (i.e., that remaining after dissipation) can be equated to the downward wind-energy flux at 10 m. He therefore parameterizes G*- D*, rather than simply G* as in Kraus & Turner. It is possible that dissipation could vary with the inertial oscillations but it seems unlikely that this would damp out completely the inertial variations in G*. We must, therefore, draw a similar conclusion as for the Kraus & Turner parameterization and assume that since G*- D* was set to a constant, the inertial oscillations contributing to G*, as represented by Eq. 30, were implicitely ignored by Denman.

Regarding the above mentioned anomaly in m, Niiler *[6]*, whose model we shall discuss later, argued that in Denman & Miyake's OWS PAPA data *[14]* the deepening observed was not caused by inertial oscillations because the starting depth for the mixed layer was already greater than the depth for which such mixing could be responsible. He argued that this was not the case in the data used by Turner and so could account for the more rapid deepening and resulting higher estimates for m. On the other hand, Martin and Thompson *[15]*, whose model will be discussed in Ch. 9, do not find from their experiments that Niiler's wind-wave source of turbulent energy is in fact necessary to explain observed mixed-layer deepening.

4 POLLARD, RHINES, & THOMPSON MODEL (1973)

The main achievement of the model due to Pollard, Rhines & Thompson *[5]*, henceforth denoted PRT, was to isolate a new mechanism for deepening the mixed layer. In this model it is proposed that the mixed layer moves approximately as a slab, sliding over the stratified water beneath and creating shear instability at the interface. The main function of the wind is to create mean-flow energy, up to a quarter of which then becomes available for increasing the layer potential energy through turbulent mixing at the lower entrainment interface. The pattern of flow developing is one of strong inertial motions initiated by a high wind, which itself may have only a short duration. It is implicitely assumed that any shear production of energy within the top boundary layer [i.e. that assumed to be the main mixing energy source in the Kraus & Turner (Ch. 2) and Denman (Ch. 3) models] is completely dissipated. Indeed, in their idealized model, PRT assume that this is the only dissipation occurring within the layer.

Most of the deepening is predicted to occur within the first half inertial cycle, during which the slab energy has built up to its maximum. Since the layer cannot "unmix", the potential energy, and hence the layer depth, remains approximately constant thereafter.

In terms of the mixed-layer equations of Ch. 1, the PRT model can be developed in the following way. The momentum equation (Eq. 10), which has the solution

$$\underline{\bar{u}}_b = \frac{\underline{\bar{\tau}}}{f\bar{\rho}_o h} \, (\sin(ft), \cos(ft-1)), \qquad \text{(Eq. 31)}$$

is used together with the mass conservation equation (Eq. 5) in its time-integrated form (compare with Eq. 17)

$$h\bar{\rho}_o - \int_o^t \bar{\rho}_{-h-\delta} \frac{\partial h}{\partial t} \, dt + \int_o^t \left[\frac{\alpha}{c} I_o(1-e^{-\gamma h}) + (\overline{w'\rho'})_o\right] dt = 0 \qquad \text{(Eq.32)}$$

and the system is closed either by stipulating that the overall Richardson number is equal to unity for marginal instability

$$R_i = -gh \frac{(\bar{\rho}_o - \bar{\rho}_{-h-\delta})}{\bar{\rho}_o \, \underline{\bar{u}}_b \cdot \underline{\bar{u}}_b} = 1 \qquad \text{(Eq. 33)}$$

or by assuming the energy balance (Eq. 12) to be adequately represented by

$$\frac{\partial}{\partial t} \overline{PE} + \frac{\partial}{\partial t} \overline{KE}_m - \underline{\bar{u}}_b \cdot \underline{\bar{\tau}}_o = 0. \qquad \text{(Eq. 34)}$$

We will comment on both of these 'equivalent' closing assumptions shortly, but first, to demonstrate their equivalence, we can substitute $\partial(\overline{PE})/\partial t$ from Eq. 8, estimate $\underline{\bar{u}}_b \cdot \underline{\bar{\tau}}_o$ from Eq. 10, rewrite Eq. 34 as

$$[\bar{\rho}_o \, \underline{\bar{u}}_b \cdot \underline{\bar{u}}_b + gh(\bar{\rho}_o - \bar{\rho}_{-h-\delta})] \frac{\partial h}{\partial t} - [gh(\overline{w'\rho'})_o - \frac{g\alpha h}{c} I_o] = 0, \quad \text{(Eq. 35)}$$

and then, neglecting heat exchanges with the atmosphere given by the second term, we obtain the relation of Eq. 33.

The solution for the layer depth is obtained by first writing

$$\bar{\rho}_{-h-\delta} = [z \frac{\partial \bar{\rho}}{\partial z}]_{z=-h-\delta} = [- \frac{zN^2}{g} \bar{\rho}]_{z=-h-\delta}, \quad \text{(Eq. 36)}$$

where $\frac{\partial \bar{\rho}}{\partial z}$ is the picnocline gradient, assumed to be constant, and N the Brunt-Väisälä frequency. Then substituting into Eq. 33 for $\underline{\bar{u}}_b$ and $\bar{\rho}_o$, obtained from Eqs. 31 and 32 respectively, and once again neglecting heat exchanges with the atmosphere, gives

$$h = (\frac{\bar{\tau}}{\bar{\rho}_o})^{\frac{1}{2}} \left[\frac{4(1-\cos ft)}{f^2 N^2} \right]^{1/4} . \quad \text{(Eq. 37)}$$

For small time $(1-\cos ft) \approx \frac{(ft)^2}{2}$ and Eq. 37 reduces to

$$h = 2^{1/4} \left(\frac{\tau}{\bar{\rho}_o N} \right)^{\frac{1}{2}} t^{\frac{1}{2}} , \quad \text{(Eq. 38)}$$

which is shown by PRT to be in good agreement with the laboratory experiments of Kato & Phillips *[11]*.

To show this agreement PRT first corrected Kato & Phillips' experimental data to account for such effects as the depth of the stirring grid below the free surface, the momentum absorbed by the water throughout this depth, and the time taken for the grid to reach full inertia. The discrepancy rationalized by Kato & Phillips to account for the original experimental data is explained by pointing to errors in the rationalization used. For example, Kato & Phillips assumed that the friction velocity u_* could be used to represent the turbulent velocity $|u'|$, which may not be the case, and, more seriously, although they used salt stratification in their experiment they cited Turner's *[16]* results for heat stratification. Had they used the salt stratification results, an $h \propto t^{1/4}$ dependence would have been deduced that clearly would have deviated from their data.

The undesirable aspects of the PRT model, apart from the assumption of slab-like flow while applying a constant wind stress, are in the assumptions that: 1) all the energy produced by wind-induced shear is dissipated, 2) no dissipation occurs at the lower interface production zone, and

3) the condition for marginal stability at the lower interface depends on a bulk Richardson number using length scales of the order of the mixed-layer depth.

The first of these assumptions is considered by Niiler *[6]* to be incorrect and in his treatment he allows only a fixed fraction of this energy to be dissipated while the remainder becomes available for mixing. Niiler also allows for some dissipation at the lower interface (assumption 2 above) through introduction into the mean momentum balance of a drag force for the inertial oscillations. As may be deduced from Niiler & Kraus *[1]*, however, this term probably has more to do with radiation of energy away from the lower interface by internal waves than with dissipation of energy. Nevertheless, Wyatt's criticism *[17]* of Niiler's model does not take this drag-force term into account. Wyatt, instead, develops two variations on PRT's model. The first parameterizes into dissipation a fixed fraction of the combined upper-wind-induced and lower-interface-production energies while the second makes the same parameterization but allows the parameter to vary in time according to PRT's Richardson-number stability constraint. These approaches will be discussed in more detail in Ch. 7.

The third of the above assumptions is considered in some detail by Wyatt who, after studying films of an entrainment interface taken by Kantha *[18]*, came to the conclusion that the appropriate Richardson number for marginal instability depends not on the mixed-layer depth, but on a length scale that varies randomly in time, this length scale being related to the scale of distortions caused by growing instabilities at the interface. It was suggested, although measurements were not available in support, that the length scale should be related to the region of velocity variation. We note, however, that using smaller values of the critical Richardson number defined by Eq. 33 as a way of accounting for a smaller relevant length scale, Wyatt did not find much variation in predicted mixed-layer depths when using her version of the PRT model.

5 NIILER MODEL (1975)

The model due to Niiler *[6]* is effectively a combination of the models due to Kraus & Truner *[4]* (or Denman *[8]*) and PRT *[5]*. It predicts a strong influence by inertial oscillations on the mixed-layer depth over a time scale $N^{-1} < t < f^{-1}$. On both smaller and larger time scales the shear production of turbulent energy in the surface wind-wave driven layer dominates.

Niiler's treatment emphasizes the separation of the mixed layer into the three distinctive sublayers described earlier and shown in Fig. 1. By making the assumptions that the upper and lower shear layers are thin compared with the mixed-layer depth and that the Reynolds shear stress in the upper layer and the mean velocity gradient in the lower layer are approximately constant, the shear production term in the turbulent energy balance (Eq. 2) can be approximated by upper and lower contributions as (see App. A)

$$\int_{-H}^{0} \bar{\rho}_o \, \overline{(\underline{u}'w')} \cdot \frac{\partial \bar{\underline{u}}}{\partial z} \, dz = -(\bar{\underline{u}}_o - \bar{\underline{u}}_b) \cdot \underline{\tau} - \frac{\rho_o}{2} \bar{\underline{u}}_b \cdot \bar{\underline{u}}_b \frac{\partial h}{\partial t} \quad . \qquad \text{(Eq. 39)}$$

The slab-flow approximation has of course been used here, so that there is no contribution to shear production throughout the bulk of the mixed layer. Niiler does point out, however, that if a velocity difference of only 0.1m/s existed across the mixed layer, shear production could indeed become important there.

Using Eqs. 3 and 6 to eliminate the mass-flux term, neglecting the time rate of change of turbulent energy, and using Eq. 39 for the shear production, the turbulent-energy balance Eq. 2 can be written

$$-\frac{\bar{\underline{u}}_b \cdot \bar{\underline{u}}_b}{2} \frac{\partial h}{\partial t} - \cancel{g}gh(\bar{\rho}_o - \bar{\rho}_{-h-\delta}) \frac{\partial h}{\partial t} - g\frac{h^2}{2} \frac{\partial \rho_o}{\partial t} - \frac{g\alpha}{c} I_o$$

$$= (\bar{\underline{u}}_o - \bar{\underline{u}}_b) \cdot \bar{\underline{\tau}}_o - [\overline{w'p'} + \overline{w'KE'}_t]_o - \varepsilon \quad . \qquad \text{(Eq. 40)}$$

The solar-heating contribution in $e^{-\gamma h}$ has been neglected in Eq. 40. If now we consider only temperature effects on density, write

$$\theta = \frac{c}{\alpha} [\bar{\rho}_o h - \frac{h}{2} \bar{\rho}_{-h-\delta}] \qquad \text{(Eq. 41)}$$

for the heat content of the water column, and use Eq. 36 to represent $\bar{\rho}_{-h-\delta}$, the bulk mass conservation Eqs. 5 and 7 take the form

$$\frac{\partial\theta}{\partial t} = \frac{c}{\alpha}\left[\bar{\rho}_o \frac{\partial h}{\partial t} + h \frac{\partial \bar{\rho}_o}{\partial t} + \frac{\partial \bar{\rho}}{\partial z} h \frac{\partial h}{\partial t}\right]$$

$$= -\frac{c}{\alpha}\left(\overline{w'\rho'}\right)_o - I_o(1-e^{-\gamma h})$$

$$= -\dot{Q}_o \text{ , say ,} \qquad \text{(Eq. 42)}$$

where $\dot{Q}_o$ represents the rate of heat exchange with the atmosphere across the air/sea interface. Then by use of Eqs. 41, 42, and 36, the turbulent energy balance of Eq. 40 takes the form

$$\frac{\partial h}{\partial t}\left[-\frac{\alpha g}{2c\rho_o}\theta + N^2\frac{h^2}{4} - \frac{1}{2}\,\bar{\underline{u}}_b \cdot \bar{\underline{u}}_b\right]$$

$$= \{(\bar{\underline{u}}_o - \bar{\underline{u}}_b)\cdot\bar{\underline{\tau}}_o - [\overline{w'p'} + \overline{w'\,KE'}_t]_o - \varepsilon\} - \frac{gh\alpha\dot{Q}_o}{2c\rho_o} \,. \qquad \text{(Eq. 43)}$$

The second term on the right of Eq. 43 is the rate at which kinetic energy within the top shear layer becomes available for mixing and, as in Denman *[8]*, Niiler parameterizes this quantity as a constant fraction m_o of the downward wind-energy flux $U_{10}|\bar{\underline{\tau}}|$ at 10 metres. We recall (see Eqs. 26 and 29 that Denman *[8]* did not reduce this term to its present form before parameterization and so implicitly included the contribution $\frac{1}{2}\bar{\underline{u}}_b\,\bar{\underline{u}}_b\frac{\partial h}{\partial t}$ from the lower boundary, which in Eq. 43 has been separated out to be dealt with in another way. The fraction m_o was chosen by Niiler to correspond to the true fraction scaled relative to the theoretically derived fraction $(C_{10}\rho a/\rho_o)^{1/2}$, itself based on the assumption (see Eqs. 27 & 28) that the available mixing energy is equal to $u_*|\bar{\underline{\tau}}|$. Thus

$$(\bar{\underline{u}}_o - \bar{\underline{u}}_b)\cdot\bar{\underline{\tau}} - [\overline{w'p'} + \overline{w'KE'}_t]_o - \varepsilon$$

$$= m\,U_{10}|\bar{\underline{\tau}}|$$

$$= m_o(C_{10}\rho a/\rho_o)^{1/2}\,U_{10}|\bar{\underline{\tau}}|$$

$$= m_o\,u_*|\bar{\underline{\tau}}| \,. \qquad \text{(Eq. 44)}$$

This alternative scaling has no significance, however, other than to make m_o an order-one quantity.

To close Eqs. 42 and 43, Niiler uses the momentum balance of Eq. 10, modified to include the loss of momentum radiated from the bottom of the layer by internal waves, as

$$\frac{\partial}{\partial t}(h\,\underline{\bar{u}}_b) + \underline{f} \times h\,\underline{\bar{u}}_b = \frac{\bar{\tau}_o}{\rho_o} - C_D|\underline{\bar{u}}_b|\,\underline{\bar{u}}_b \quad , \qquad \text{(Eq. 45)}$$

where C_D is a drag coefficient.

Equations 42, 43, and 45 then form the basic equations for Niiler's model.

The small-time $(t < N^{-1})$ solution

$$h \sim (12\,m_o)^{1/3}\left(\frac{\tau_o}{\rho_o N}\right)^{1/3}(tN)^{1/3} \qquad \text{(Eq. 46)}$$

was derived analytically by setting the surface heating $\dot{Q}_o$ and the drag coefficient C_D equal to zero.

Using constant values of m_o, Q_o, and C_D, numerical solutions were derived and shown to display the following general characteristics:

1) For large times of $t >> f^{-1}$ the layer depth was found to approach the value

$$h \to 2\,m_o\left(\frac{\tau_o}{\rho_o}\right)^{3/2}\frac{\rho_o c}{\dot{Q}_o g\alpha}$$

2) The surface production of energy dominated the lower interface production not only for times of $t < N^{-1}$ but also for $t > f^{-1}$

3) If the initial layer depth was greater than $2\,\tau_o^{1/2}(\rho_o N f)^{-1/2}$, deepening was caused solely by surface processes.

4) The inertial oscillations, through energy production at the lower interface, caused rapid deepening for times $N^{-1} < t < f^{-1}$ but for sufficiently large times $(t >> f^{-1})$ the same eventual depth was found to result without inertial oscillations.

5) Without surface heating $(\dot{Q}_o = 0)$ the layer was found to deepen without bound according to the small-time solution of Eq. 46.

The main weak point of Niiler's model, again apart from the slab-flow assumption common to all such models, is in its treatment of mechanical dissipation of energy. As mentioned earlier, Wyatt *[17]* has pointed out that all of the dissipation in Niilers' model occurs within the upper shear

layer and none within the lower interface layer. In view of parameterization (Eq. 44), however, her comment that a value of m_o exceeding unity would imply negative dissipation appears to be unfounded. Some allowance for dissipation of the lower interface is tentatively made by Niiler in his drag force parameter C_D, although this term is more fundamentally concerned with radiation of energy away from the production zone by interval waves. The importance of dissipation was later recognized by Niiler in the review by Niiler & Kraus *[1]*. There dissipation was divided into three separate contributions arising as specified fractions of each of the mixing-energy sources: upper shear-layer production, lower interface shear production due to the inertially oscillating mean flow, and convective release due to surface cooling. Niiler & Kraus also proposed that these fractions be allowed to vary in time such that the predominating energy production mechanism be brought into balance with dissipation as $h \to h_\infty$.

6 NON-INTEGRAL MODELS

6.1 Mellor & Durbin Model (1975)

All bulk mixed-layer models suffer from the assumption they must make regarding an imposed mixed-layer geometry. A mixed layer is thus not a prediction of the models but an a priori assumption. The model due to Mellor & Durbin (henceforth referred to as MD) *[19]* is of great qualitative interest, therefore, since not being an integral model it does not need to make this imposing assumption. It has been used to add authenticity, for example, to bulk-model results by Wyatt *[17]* and by Martin & Thompson (henceforth referred to as MT) *[15]*, both with qualified success.

After making corrections to their computer program, Wyatt found a certain qualitative agreement between the MD results and her own bulk-model results but found that the mixed-layer depths predicted by the former were consistently under estimated. MT, on the other hand, found that over time scales greater than about one week, agreement with their three-layer bulk model was good. We will comment further on these important comparisons later but first it is appropriate to present a brief summary of the MD model.

The approach adopted is similar to that of Munk & Anderson *[20]* in that the one-dimensional momentum and heat equations are solved after parameterizing the turbulent velocity and heat fluctuation in the interior by use of eddy viscosity coefficients.

The equations are

$$\frac{\partial \bar{\underline{u}}}{\partial t} + f \times \bar{\underline{u}} + \frac{\partial}{\partial z}\left[\overline{\underline{u}'w'} - \nu \frac{\partial \bar{\underline{u}}}{\partial z}\right] = 0 \qquad \text{(Eq. 47)}$$

and

$$\frac{\partial \bar{T}}{\partial t} + \bar{w}\frac{\partial \bar{T}}{\partial z} + \frac{\partial}{\partial z}\left[\overline{T'w'} - \nu_t \frac{\partial \bar{T}}{\partial z}\right] = 0 \ , \qquad \text{(Eq. 48)}$$

where ν and ν_T are molecular diffusion coefficients which, although small, are included for numerical reasons. The turbulence terms are parameterized after Mellor & Yamada *[21]* in the form

$$-\overline{\underline{u}'w'} = \ell_q S_m \frac{\partial \bar{\underline{u}}}{\partial z}$$

and

$$-\overline{T'w'} = \ell_q S_H \frac{\partial \bar{T}}{\partial z} \ , \qquad \text{(Eq. 49)}$$

where S_M and S_H are complicated functions of the flux Richardson number and universal empirical parameters drawn from a bank of neutral turbulent flow data, q is the rms turbulent velocity calculated from the steady-state

turbulent energy equation (cast in a form involving another empirical constant), and ℓ is a length scale estimated from

$$\ell = \frac{Kz}{1 + Kz/\ell_\infty} \qquad \text{(Eq. 50)}$$

$$\ell_\infty = m_1 \frac{\int_{-\infty}^{0} qz\, dz}{\int_{-\infty}^{0} q\, dz} ,$$

with m_1 yet another empirical constant. In fact MD used only ℓ_∞, which, as proposed by Wyatt, could be a reason for very little surface production of energy in their model.

Solutions to Eqs. 47 and 48 are obtained by integration in time. At each time step the turbulent fluxes are calculated by iteration between Eq. 49, Eq. 50 and the expressions for S_M, S_N, the flux Richardson number, and the turbulent energy equation in q.

Although a large number of empirically derived constants are required by the above approach, these constants are fairly well established by previous experimental work. A question remains, however, as to their validity in the open ocean. Wyatt, for example, believes that certain of the empirical parameters in the calculations of S_M and S_N are not valid in the ocean.

Results from the model show that the mean velocity does not become uniform with depth unless the wind is turned off. In that case the velocity shear disappears within 0.2 of an inertial period. The layer was found to deepen most rapidly during the first inertial period and continue to deepen, though progressively less rapidly, for remaining oscillations. Quite good agreement was reported between the model output and OWS PAPA *[14, 22]*. However, in view of MD's claim not to have adjusted constants in their model to obtain better agreement with the data and since their model results are quantitatively incorrect by up to 30% because of a programming error pointed out by Wyatt, doubt must be cast on the initial choice of constants and parameters, including possibly the surface-drag coefficient. Wyatt found best quantitative agreement between her model (to be summarized in Ch. 7) and that of MD if a rather low critical Richardson number (Ri=0.25) was chosen to represent marginal stability. In comparisons with JASIN data *[23]* collected in the Western N. Atlantic, Wyatt found that Richardson numbers did not fall below 1 and so the MD model consistently under-predicted the mixed-layer depth. Correction of the earlier mentioned length scale from ℓ_∞ to ℓ (Eq. 50), thus increasing the surface shear production of energy, did not apparently improve the predictions.

Martin and Thompson's (to be summarized in Ch. 8) comparison of their model with that of MD showed quite good agreement between the predicted mixed-layer depths, provided that a sufficiently long integration time and strong initial stratification were used. The two predictions were found to converge to the same value after about one week. It is worth pointing out, perhaps, that the comparisons carried out by Wyatt were for shorter integration times (up to only three inertial periods) and did not allow for

surface heat exchanges. It is also of interest that MT did not allow for any surface production of the mixing energy that Wyatt had shown to be important in explaining JASIN data.

The good agreement found by MT between the MD model and ensemble-averaged data taken from OWS NOVEMBER in the north Pacific was for seasonal variations – again on a much larger time scale than that considered by Wyatt.

Before returning to discuss a number of other bulk models, mention must be made of two more non-integral models.

6.2 Marchuk et al Model (1977)

The approach taken by Marchuk et al *[24]* can be distinguished from that of MD in its more complete treatment of the dynamic turbulence equations. They do not, for example, parameterize the turbulent viscosity coefficients in terms of the Richardson number but rather solve for them by using the unsteady turbulent energy generation and decay equations closed by use of an empirical formula. Marchuk et al tested their model against the observational data of Halpern *[25]* and found good agreement between predicted and measured parameters, mentioning in particular layer depth, current shear across the transition zone, changes in current due to storm, estimated turbulent viscosity coefficients, and estimated Richardson numbers. Examining the velocity profiles in Marchuk et al, however, shows a somewhat large vertical shear within the mixed layer, both before and during the passage of a storm. This is not consistent with bulk-model assumptions.

6.3 Warn-Varnas and Piascek Model (1979)

The model by Warn-Varnas & Piascek *[26]* is an example of a higher-order turbulence closure technique described by Mellor & Yamada *[21]*. Rather than parameterizing the effects of the triple correlation terms as has been done in earlier models (e.g. Garwood, *[7]*) the terms become variables in a higher-order set of equations. In these equations fourth-order correlation terms are parameterized using various empirical constants. In fact this approach involves the use of a rather larger number of empirically determined constants than is needed in simpler models.

Determination of the relevant length scale, which is important in modelling the higher-order correlation terms, requires the use of yet another empirical constant.

Running their model, Warn-Varnas and Piascek show the mixed-layer depth to be three times greater when including the triple correlation terms, yet when comparing their model with that of Mellor & Durbin *[19]* their mixed-layer depths were found to be only 10% greater. They suggest that the much larger length scale chosen by Mellor and Derbin served to compensate for the deepening effect of the triple correlation terms neglected.

7 WYATT MODEL (1976)

The model most preferred by Wyatt *[17]* in her extensive comparisons between existing models and those modified and improved by herself is the one she refers to as PW. We will therefore discuss only this model here. The model derivation will not, however, be presented here since PW is effectively a combination of the models due to Denman *[8]* and Pollard et al *[5]*, both presented earlier. Because of this combination, the model is closely related to, and so is to be compared with, that of Niiler *[6]*, also presented earlier. The model carefully distinguishes between two lower-interface production mechanisms: shear-flow instability, modelled after PRT using a bulk Richardson number criterion, and steady shear production of turbulence modelled by use of the turbulent kinetic energy balance.

Wyatt argues that Niiler's (1975) model does not take into account any dissipation of turbulent energy produced by the mean flow shear at the mixed-layer/thermocline interface. Instead, all of this dissipation is implied to occur within the top wind-wave shear layer. It was proposed by Wyatt that dissipation should occur as a constant fraction of turbulent production within each of the upper and lower shear layers. In this case, and assuming a slab-flow approximation for Denman's (1973) model, the turbulent energy equation (Eq. 2) is written in the form

$$\frac{\partial}{\partial t}\overline{PE} = \left\{ \overline{\underline{\tau}}_o \cdot (\overline{\underline{u}}_o - \overline{\underline{u}}_b) + \tfrac{1}{2}\, \overline{\underline{u}}_b \cdot \overline{\underline{u}}_b \frac{\partial h}{\partial t} \right\}$$

$$-(1-m_w)\left\{ \underline{\tau}_o \cdot (\overline{\underline{u}}_o - \overline{\underline{u}}_b) + \tfrac{1}{2}\, \overline{\underline{u}}_b \cdot \overline{\underline{u}}_b \frac{\partial h}{\partial t} \right\}, \qquad \text{(Eq. 51)}$$

where the first term was obtained by substituting Eq. 3 into Eq. 2, neglecting the solar input I_o, and the second term by substituting into Eq. 2 the upper and lower shear production contributions given by Eq. 39. The third term formulates the assumption that a fixed fraction of the production is lost to dissipation. The turbulent tendency term $\frac{\partial}{\partial t}\overline{KE}_t$ and the surface kinetic-energy flux term $[\overline{w'p'} + \overline{w'KE'_t}]_o$ were both neglected in Eq. 51.

Next, as first suggested by Turner *[13]*, it is assumed that the surface production rate $\overline{\underline{\tau}}_o \cdot (\overline{\underline{u}}_o - \overline{\underline{u}}_b)$ can be parameterized as a constant fraction K of the downward wind-energy flux at 10 m. Thus Eq. 51 is rewritten as

$$\frac{\partial}{\partial t}\overline{PE} = [m_w\, kU_{10} + IP], \qquad \text{(Eq. 52)}$$

where IP is a label for the interface production term $\frac{1}{2}\, \overline{\underline{u}}_b \cdot \overline{\underline{u}}_b \frac{\partial h}{\partial t}$. In this formulation the fraction of the wind energy flux at 10 m actually

available for mixing is equal to $m_w k$. This is to be compared with the parameter m of Eq. 44 in our description of Niiler's model. The term IP in Eq. 52 is calculated using the slab momentum balance equation (Eq. 10).

The energy balance (Eq. 52) actually defines a model called DW by Wyatt. Model PW was obtained by applying DW until the bulk Richardson number

$$R_i = -gh \frac{(\bar{\rho}_o - \bar{\rho}_{-h-\delta})}{\bar{\rho}_o \, \underline{\bar{u}}_b \cdot \underline{\bar{u}}_b} \qquad \text{(Eq. 53)}$$

fell below a critical value of 1, say. In this case the energy equation (Eq. 52) was replaced by the Richardson number (Eq. 53) (set to its critical value) as the closing assumption. Deepening was thus assumed to be controlled by a stability parameter in this way until Eq. 52 indicated that the Richardson number was no longer critical. The layer was found to deepen much faster during the period of marginal instability and, assuming that the energy balance must remain satisfied, calculations by substituting Eq. 53 in Eq. 52 showed that the proportion of mixing energy dissipated during this period was much higher. PW, then, was effectively the application of Eq. 52, but with m_w varying in time according to the value of a stability parameter.

A critical value of $R_i = 1$ was chosen by PRT to represent marginal stability. This value was also used by Wyatt, but other lower critical values were tried in an attempt to recognize that h in the definition of Eq. 49 was not really the appropriate length scale. The appropriate length scale, it was proposed, should be related to the thickness of the mean-velocity shear layer, but since this was unknown a more rigorous treatment was not attempted.

In model comparisons with JASIN data *[23]* Wyatt found that the critical Richardson number was consistently above 1, and so the tested model PW effectively became the model DW. By a suitable choice of m_w and K the model DW was found to give the best fit to the data. Also, as mentioned earlier, the model was found to give better predictions than the MD model (Sect. 6.1). For this particular data set, surface production of energy was found to dominate over lower-interface production to the extent that a Denman model (Ch. 3) would also have been a reasonable approximation.

8 GARWOOD MODEL (1977)

In the model by Garwood *[7]*, entrainment at the lower interface and hence layer deepening is controlled by a parameter expressing the ratio of buoyant damping to the convergence of turbulent kinetic energy at the interface

$$m_4 = \frac{-\frac{g}{\rho_o}\overline{\rho' w'}}{\frac{\partial}{\partial z}\left(\overline{w' KE'_t} + \frac{\overline{w' p'}}{\rho_o}\right)} . \qquad \text{(Eq. 54)}$$

This contrasts with the more commonly used gradient Richardson number, which expresses the ratio of buoyant damping to the production of turbulent kinetic energy within the entrainment zone. Garwood considers such production to be insignificant when compared with the local convergence of turbulent energy. Using the dimensionally derived turbulent-transport time scale

$$\tau_e = a_1 h \overline{\langle w'^2 \rangle}^{-\frac{1}{2}} , \qquad \text{(Eq. 55)}$$

with a_1 a constant of proportionality such that

$$-\frac{\partial}{\partial z}\left(\overline{w' KE'}_t + \frac{\overline{w' p'}}{\rho_o}\right) = \frac{\langle \overline{KE}_t \rangle}{\tau_e} , \qquad \text{(Eq. 56)}$$

where the angle brackets '$\langle\ \rangle$' represent vertical averages. Such averages are to be distinguished from the earlier defined bulk values $(\ )_b$, since in the latter it was assumed that the variable was approximately uniform throughout the mixed layer. Combining Eqs. 54, 55, and 56 yields, for the entrainment mass flux,

$$\frac{g}{\rho_o}(\overline{\rho' w'})_{-h} = \frac{m_4 \langle \overline{w'^2} \rangle^{\frac{1}{2}} \langle \overline{KE}_t \rangle}{h} \qquad \text{(Eq. 57)}$$

Also required for the model are the usual bottom boundary conditions or specific jump equations (Eqs. 7 and 11) describing the mass and momentum fluxes across the entrainment interface. These take the forms

$$-(\overline{w' \rho'})_{-h} = (\langle \overline{\rho} \rangle - \overline{\rho}_{-h-\delta}) \frac{\partial h}{\partial t} \qquad \text{(Eq. 58)}$$

$$-(\overline{u' w'})_{-h} = (\langle \underline{\overline{u}} \rangle - \underline{\overline{u}}_{-h-\delta}) \frac{\partial h}{\partial t} . \qquad \text{(Eq. 59)}$$

We note that some error is likely in using these relations, since the quantities $\langle\bar{\rho}\rangle - \bar{\rho}_{-h-\delta}$ and $\langle\underline{\bar{u}}\rangle - \underline{\bar{u}}_{-h-\delta}$ are assumed to represent the jumps in density and velocity respectively across the entrainment zone. For the density this assumption is reasonable, but since velocity shear is allowed here to exist throughout the mixed layer the velocity jump across the entrainment zone ought to be considerably less.

In common with Pollard, Rhines & Thompson *[5]* and with Niiler *[6]*, the model requires the mass-conservation and horizontal-momentum balances of Eqs. 5 and 10, which we rewrite here by use of Eqs. 58 and 59 as

$$h\frac{\partial}{\partial t}\langle\bar{\rho}\rangle + (\langle\bar{\rho}\rangle - \bar{\rho}_{-h-\delta})\frac{\partial h}{\partial t} + (\overline{w'\rho'})_o + \frac{\alpha I_o}{c} = 0 \qquad \text{(Eq. 60)}$$

and

$$h\frac{\partial}{\partial t}\langle\underline{\bar{u}}\rangle + (\langle\underline{\bar{u}}\rangle - \underline{\bar{u}}_{-h-\delta})\frac{\partial h}{\partial t} + (\overline{\underline{u}'w'})_o + h(f\times\langle\underline{\bar{u}}\rangle) = 0. \qquad \text{(Eq. 61)}$$

Also in common with Niiler *[6]* the problem is now closed by modelling the turbulent kinetic-energy equation. Here, however, the treatment is novel and more rigorous than in previous models. The energy balance is first divided into horizontal and vertical components, thus recognizing that the turbulent eddies are not isotropic. Each term of the balance is then parameterized by turbulent-field modelling techniques and, in the case of dissipation, by a judicious choice of time scales. The integrated, component, turbulent-energy, balance equations can be written as

$$\frac{\partial}{\partial t}\left(h\frac{\langle\overline{\underline{u}'.\underline{u}'}\rangle}{2}\right) + \int_{-h-\delta}^{o}\overline{\underline{u}'w'}.\frac{\partial\underline{\bar{u}}}{\partial z}\,dz + \int_{-h-\delta}^{o}\frac{\partial}{\partial z}\left(w'\frac{\overline{\underline{u}'.\underline{u}'}}{2}\right)dz$$

$$-\int_{-h-\delta}^{o}\frac{\overline{p'}}{\rho_o}\left(\frac{\partial u_1'}{\partial x_1} + \frac{\partial u_2'}{\partial x_2}\right)dz + \int_{-h-\delta}^{o}\Omega_2\,\overline{u_1'w'}\,dz$$

$$+\frac{2}{3}\int_{-h-\delta}^{o}\nu\,\overline{\frac{\partial u_i'}{\partial x_j}\frac{\partial u_j'}{\partial x_j}}\,dz = 0 \qquad \text{(Eq. 62)}$$

and

$$\frac{\partial}{\partial t}\left(h\,\overline{\langle w'\rangle^2}\right) + \int_{-h-\delta}^{o}\frac{g}{\rho_o}(\overline{w'\rho'})dz + \int_{-h-\delta}^{o}\frac{\partial}{\partial z}\left(\overline{w'^3} + \frac{\overline{w'p'}}{\rho_o}\right)dz$$

$$-\int_{-h-\delta}^{o}\overline{\frac{p'}{\rho_o}\frac{\partial w'}{\partial z}}\,dz + \int_{-h-\delta}^{o}\Omega^2\,\overline{u_1'w'}\,dz$$

$$+ \frac{1}{3} \int_{-h-\delta}^{o} \nu \overline{\frac{\partial u_i'}{\partial x_j} \frac{\partial u_i'}{\partial x_j}} \, dz = 0 \qquad \text{(Eq. 63)}$$

The shear-production term of Eq. 62 is modelled as

$$\int_{-h-\delta}^{o} (\overline{\underline{u}'w'}) \cdot \frac{\partial \overline{\underline{u}}}{\partial z} \, dz \approx - u_*^2 \, \delta \, U \, (o) + \int_{-h}^{o} \overline{\underline{u}'w'} \, \frac{\partial \overline{\underline{u}}}{\partial z} \, dz \quad , \qquad \text{(Eq. 64)}$$

where $\delta \, U(o)$ is a measure of the excess surface velocity due to shear. It is then assumed that

$$\delta \, U(o) = m_3 \, u_* \quad , \qquad \text{(Eq. 65)}$$

where m_3 is a constant to be determined, and that the integral on the right-hand side of Eq. 64 is given by (compare Eq. 39) the expression

$$- \frac{\langle \overline{\underline{u}} \rangle - \overline{\underline{u}}}{2} \, {}^{2}_{-h-\delta} \frac{\partial h}{\partial t} \quad . \qquad \text{(Eq. 66)}$$

As in Niiler [6], Garwood augments this shear production with the surface flux of turbulent kinetic energy and pressure perturbations, as represented by the third term in Eq. 62. The lower contribution of this term is associated with the radiation of energy away from the mixed layer by internal waves and is assumed to be unimportant in this model.

The surface flux of kinetic energy is thought to be caused primarily by breaking surface waves and is taken to be proportional to u_*^3 for a fully developed wave field. The constant m_3 in Eq. 65 is thus adjusted to account for breaking surface waves. A problem arising in Garwood's treatment, however, is that it is not known what proportion of the surface energy flux makes a contribution in the horizontal energy balance (Eq. 62) and what proportion makes a contribution in the vertical energy balance (Eq. 63) . Garwood's method appears to attribute the whole of this term to the former (see Garwood's equations 37 and 38).

The pressure redistribution term in Eq. 62 is rewritten as

$$\int_{-h-\delta}^{o} \overline{\frac{p'}{\rho_o} \left(\frac{\partial u_1'}{\partial x_1} + \frac{\partial u_2'}{\partial x_2} \right)} \, dz = \int_{-h-\delta}^{o} \overline{\frac{p'}{\rho_o} \frac{\partial w'}{\partial z}} \, dz$$

$$= m_2 \overline{\langle KE_t \rangle}^{\frac{1}{2}} \left(\langle KE_t \rangle - 3 \langle \overline{w'^2} \rangle \right), \qquad \text{(Eq. 67)}$$

where the first step makes use of the continuity condition $\frac{\partial u_j'}{\partial x_j} = 0$ and

the second represents a form said to be consistent with the work of Rotta *[27]* and Lumley & Khajeh-Nouri *[28]*. The constant m_2 is a parameter related to the redistribution length scale.

The net rate of dissipation is considered to have two contributions: one for shallow mixed layers where rotation is unimportant, and one for deeper mixed layers where rotation exerts a strong influence. The time scale associated with the former is assumed to be proportional to the mixed layer depth divided by the rms turbulent velocity.

$$\tau_1 = h\langle KE_t\rangle^{-\frac{1}{2}} \qquad \text{(Eq. 68)}$$

and the time scale associated with the latter is simply

$$\tau_2 = f^{-1} \qquad \text{(Eq. 69)}$$

The introduction of a rotational time scale for dissipation is a new concept in bulk mixed-layer models. It is argued that since rotation turns the mean shear direction with depth there is an inseparable link between rotation and local shear production of energy. The assumption is then made that the local rate of dissipation is related to the local rate of production. The convective and rotational time scales are combined to give a dissipation time scale τ_ε such that

$$\tau_\varepsilon^{-1} = m_1 \tau_1^{-1} + m_5 \tau_2^{-1} \quad , \qquad \text{(Eq. 70)}$$

where m_1 and m_5 are constants of proportionality.

Next, by dimensional reasoning, the net rate of dissipation is taken to equal $h\langle \overline{KE_t}\rangle \tau_\varepsilon^{-1}$, which by Eqs. 68, 69 and 70 gives

$$\int_{-h-\delta}^{o} \nu \overline{\frac{\partial u_i'}{\partial x_j}\frac{\partial u_i'}{\partial x_j}}\, dz = h\,\overline{\langle KE_t\rangle}\,\tau_\varepsilon^{-1}$$

$$= m_1 \overline{\langle KE_t\rangle}^{3/2} + m_5\, hf\overline{\langle KE_t\rangle} \, . \qquad \text{(Eq. 71)}$$

Combining the contributions of Eqs. 64, 67 and 71, the energy balance of Eq. 62 can be written as

$$\frac{\partial}{\partial t}\{h(\overline{\langle KE_t\rangle} - \overline{\langle w'^2\rangle})\} - \left\{ m_3 u_*^3 + \frac{\left(\langle \bar{u}\rangle - \bar{u}_{h-\delta}\right)^2}{2} \frac{\partial h}{\partial t} \right\}$$

$$+ \{m_2 \overline{\langle KE_t\rangle}^{\frac{1}{2}} (\overline{\langle KE_t\rangle} - 3\overline{\langle w'^2\rangle})\}$$

$$+ \frac{2}{3}\{m_1 \overline{\langle KE_t\rangle}^{3/2} + m_5 hf\overline{\langle KE_t\rangle}\} = 0 \, . \qquad \text{(Eq. 72)}$$

For the vertical balance, Eq. 63, the potential energy term is estimated either by a double integration of the mass flux, Eq. 4, or by elimination of the potential energy between Eqs. 3 and 6. Using the former method we have

$$\int_{-h-\delta}^{o} \frac{g}{\rho_o}(\overline{w'\rho'}) = \frac{g}{\rho_o}\frac{h^2}{2}\frac{\partial\langle\bar{\rho}\rangle}{\partial t} + \frac{g}{\rho_o} h(\overline{w'\rho'})_o$$

$$+ \frac{g}{\rho_o}\frac{\alpha}{c\gamma} I_o(1-\gamma^{-1}) \quad . \qquad \text{(Eq. 73)}$$

Ignoring the flux convergence term in $\frac{\partial}{\partial z}(\overline{w'^3} + \frac{\overline{w'p'}}{\rho_o})$, which was not accounted for by Garwood, neglecting the rotation redistribution term, and using Eqs. 73, 67, and 71, yields for the vertical energy balance

$$\frac{\partial}{\partial t}\{h\langle\overline{w'^2}\rangle\} + \frac{hg}{\rho_o}\left\{\frac{h}{2}\frac{\partial\langle\bar{\rho}\rangle}{\partial t} + (\overline{w'\rho'})_o + \frac{\alpha}{c} I_o(1-(h\gamma)^{-1}\right\}$$

$$- \{m_2 \langle\overline{KE_t}\rangle^{\frac{1}{2}} (\langle\overline{KE_t}\rangle - 3\langle\overline{w'^2}\rangle)\}$$

$$+ \frac{1}{3}\{ m_1 \langle\overline{KE_t}\rangle^{3/2} + m_5 hf\langle\overline{KE_t}\rangle\} = 0 \quad . \qquad \text{(Eq. 74)}$$

Equations 57 and 58 combine to give a third equation

$$(\langle\bar{\rho}\rangle - \bar{\rho}_{-h-\delta})\frac{\partial h}{\partial t} + m_4 \frac{\langle\overline{w'^2}\rangle^{\frac{1}{2}} \langle\overline{KE_t}\rangle}{h} = 0 \quad . \qquad \text{(Eq. 75)}$$

Equations 72, 74, and 75, together with the bulk mass and momentum Eqs. 60 and 61, then form a closed set of differential equations in h, $\langle\bar{\rho}\rangle$, $\langle\bar{\underline{u}}\rangle$, $\langle\overline{w'^2}\rangle$, and $\langle KE_t\rangle$. The adjustable parameters in the model are: the surface-heat flux term $(\overline{w'\rho'})_o$, the penetrating component of solar radiation I, the surface wind stress $(\overline{\underline{u}'w'})_o$, the density $\bar{\rho}_{-h-\delta}$ below the mixed layer, and the velocity $\bar{\underline{u}}_{-h-\delta}$ below the mixed layer.

By estimating approximate values for the empirical constants $m_1, m_2, \ldots m_5$ and choosing hypothetical values for the adjustable parameters, Garwood explores the general behaviour of the model. The important non-dimensional parameters turn out to be a mixed-layer stability parameter H^* expressing the ratio of the effective buoyancy flux to the input of mechanical energy by the wind, an interface stability parameter P^* measuring the entrainment rate, and a parameter Z^* related to the mixed-layer depth.

These are written

$$H^* = \frac{hg}{\rho_o} \{(\overline{w'\rho'})_o + \frac{\alpha}{c} I_o(1-(h\gamma)^{-1})\}/2\, m_3 u_*^3$$

$$P^* = \frac{hg}{\rho_o} (\overline{w'\rho'})_{-h}/2\, m_3 u_*^3$$

$$Z^* = \frac{m_5}{m_1} \frac{hf}{u_*} \quad .$$

It is found that the rate of entrainment P^* decreases with the mixed-layer depth Z^* and that in the retreat mode ($P^* = 0$) the maximum stability H^*max is not constant as in other models but is a function of Z^* (i.e. layer depth, rotation, and wind stress).

The ability of the model to predict a cyclic steady state on an annual scale is demonstrated by using a sinusoidal surface-buyoyancy flux and a constant wind stress. This takes the form of a closed loop in the Z^* - H^* plane. Such a cyclic state is possible because dissipation for deeper mixed layers is enhanced by planetary rotation, which is assumed to influence the turbulence-dissipation time scale.

Another distinguishing feature of the model is in its prediction of a non-linear dependence of the entrainment rate P^* on layer stability H^*.

Finally, it is suggested that plots in the Z^*-H^*-P^* space can be used in general as a bases for comparison between the various models.

Although Garwood's model requires the use of five empirical constants whose values might be both difficult to measure in the open ocean and subject to some variation from one experiment to another, such a model, with each contribution to the generation and dissipation of mixing energy parameterized separately, offers a great versatility in application. On the other hand, the sensitivity of the model to the values of the five constants has not been presented and if the model is sensitive over the expected range of variation in the constants it might be said that this sort of model is unnecessarily complicated.

9 MARTIN & THOMPSON MODEL (1979)

The most recent model to be formulated is by Martin & Thompson *[15]*, hereafter referred to as MT. It is a three-layer upper-ocean bulk model comprising a mixed layer, a thermocline layer, and a deep layer. The reason for including the lower layers was to allow for horizontal advection effects in a later installation of the model as part of a three-dimensional numerical ocean model.

The mixed layer is assumed to move as a slab and its deepening rate to be controlled by one of two mechanisms. The first is stratification-limited deepening, in which case the model of PRT (Ch. 4) is used, with deepening controlled by a stability parameter in the form of a bulk Richardson number (see Eq. 53 or 33). The preference for depths predicted by the PRT model is based on their good approximation to those predicted by numerical integration of the Mellor & Yamada level-2 model *[21]* (henceforth referred to as the MYL2 model). The MYL2 model (presented by MD) was taken by MT, after testing against data and other theoretical considerations, to be the ideal mixed-layer model. We note however, that this view is not shared by Wyatt *[17]*, by Niiler & Krauss *[1]*, nor by Garwood *[7]*.

The second mechanism is a heat-flux-limited regime where deepening is controlled by a dimensionless parameter

$$\phi = -\frac{\alpha g Q}{f\, u_*^2} \qquad \text{(Eq. 76)}$$

expressing the ratio of the Monin - Obukov and Ekman-layer scale lengths, where Q is the surface-heat flux minus the vertically integrated penetrating component of solar radiation. The appropriate layer depth is expressed by the form *[18]*.

$$h = \frac{u_*}{f}\, h'(\phi) \quad ,$$

where h' represents a function in ϕ and is determined from numerical experiments using the MYL2 model.

The temperature (density), depth, and mean flow velocity of each of the three layers in the MT model are determined by use of one or other of the above deepening mechanisms for the mixed layer, together with application to each layer of the following bulk-momentum and heat-balance equations:

$$\frac{\partial}{\partial t}(h^i \underline{\bar{u}}^i) + f \times h^i \underline{\bar{u}}^i - \left[\nu_m \frac{\partial \underline{\bar{u}}}{\partial z}\right]_{i+\frac{1}{2}}^{i-\frac{1}{2}} - \delta_{i1} \frac{\underline{\bar{\tau}}_o}{\rho} = 0$$

$$\frac{\partial}{\partial}(h^i \bar{T}^i) + h^i I^i - \left[\nu_H \frac{\partial \bar{T}}{\partial z}\right]_{i+\frac{1}{2}}^{i-\frac{1}{2}} + \delta_{i1} \frac{Q_o}{\rho c} = 0 \quad , \qquad \text{(Eq. 77)}$$

where the subscript i refers to the layer number, ν_m & ν_H are molecular-viscosity coefficients included mainly for numerical reasons, and Q_o is the surface heat flux. The subscripts $i-\frac{1}{2}$ and $i+\frac{1}{2}$ refer to the upper and lower boundaries of the i^{th} layer.

For momentum and heat-balance calculations within the thermocline and deep layers, only the vertically averaged velocity and temperature are of interest. The vertical temperature distribution within the thermocline layer must still be retained, however, since it is important in the calculation of h for the stratification-limited regime.

In a comparative test between this model and the MYL2 model it was found that for the stratification-limited regime, and particularly for weak stratification, the PRT model predicted deeper mixed layers, with a convergence of the two after many days. To some extent this is consistent with the findings of Wyatt *[17]* although surface heating was not considered in her model. She did find, though, that wind mixing through surface production was important – a mechanism not considered to be necessary in the MT model. Had the mechanism been employed, as it should have been to be consistent with the MYL2 model, which did employ it, the discrepancies between the MT and MYL2 models would perhaps have been greater.

In the heat-flux-limited regime, agreement was somewhat better, with convergence of the two models (MT and MYL2) after about five days. Agreement was less good for low values of surface heat flux.

The models were compared with the north Pacific OWS November data. Predicted mixed-layer depths were reported to be consistently less than those observed over the one-year period. The following explanations were offered for these differences:

1) Ensemble-averaged winds were used as input to the model, thereby not accounting properly for the non-linear response of layer depth to wind speed. (i.e. the layer deepens more rapidly for high winds but does not shallow again for light ones).

2) The ensemble for the wind data was different from, although overlapping, the ensemble for the oceanographic data with which the predictions were compared.

While these explanations appear acceptable, they remain to be tested in some way before the MT model, based on the PRT model, can be said to be the best available.

CONCLUSION

Each of the models presented has been developed from the same set of basic equations, using a consistent notation throughout.

Three distinct mechanisms for the production of mixing energy appear to have emerged:

1) Surface production.
2) Shear production at the thermocline mixed-layer interface by the action of the turbulent Reynold's stresses on the mean current shear.
3) Instability at the thermocline mixed-layer interface.

The surface-production mechanism was first considered by Kraus & Turner *[4]* who, considering it to be the only energy source, parameterized it as a fixed fraction of the downward wind-energy flux at 10 metres. The parameterization of this mechanism has remained essentially the same in later models due to Denman *[8]*, Niiler *[6]*, Wyatt *[17]*, Garwood *[7]*, Niiler & Krauss *[1]* and others, although varying degrees of emphasis have been placed on different contributing components. Niiler & Kraus, for example, emphasize the surface-energy flux term $[\overline{w'KE}_t]_o$ (see Eq. 2) with surface-shear production $\int \overline{\underline{u}'w'} \cdot \frac{\partial \underline{\bar{u}}}{\partial z}\, dz$ making a small contribution. All earlier treatments, however, reverse this emphasis, with surface-shear production playing the major role. Estimates of the parameterization factor m made from observational data vary by up to an order of magnitude, thus casting some doubt on its usefulness in a prediction model. One attempt to overcome this problem was made by Wyatt *[17]* who allowed m to vary in time according to the value of a stability parameter.

Shear production of energy at the thermocline/mixed-layer interface is represented by the integral across the interface of the term $\overline{\underline{u}'w'} \cdot \frac{\partial \underline{\bar{u}}}{\partial z}$ in Eq. 2. It was first treated explicitly by Niiler *[6]* who, following Pollard, Rhines & Thompson *[5]*, used the momentum balance within the mixed layer. Indeed, this contribution can be estimated only by use of the momentum balance, since only in this way can the important effect of the earth's rotation and hence inertial oscillations be accounted for.

The third mechanism assumes that most of the energy for deepening arises from instability at the thermocline/mixed-layer interface and can be modelled by specifying the value of a stability parameter such that marginal stability is maintained. Instabilities will last for only a relatively short time, with a rapid return to a marginally stable state. The first to introduce this hypothesis into a model were Pollard, Rhines, & Thompson *[5]*. They employed bulk-momentum equations for the mixed layer and closed the system by specifying that the value of the bulk Richardson

number be unity during deepening. This model, with its widespread appeal, has been used recently in a three-layer model by Martin & Thompson *[15]* to describe deepening in a 'stratification-limited regime'. The main difficulty in applying the mechanims is in deciding on a suitable value for the bulk Richardson number or in attempting to improve the theory by, instead, defining a local gradient Richardson number. Also the mechanism does not account for the direct flux of mixing energy through the sea surface.

In the model by Garwood *[7]*, neither the second nor third mechanisms are considered to be important in comparison with the convergence at the interface of the turbulent-energy flux produced at the surface. According to Garwood it is the ratio of buoyant damping to this term that controls the entrainment rate and hence layer deepening. Another inovation due to Garwood was to allow for an enhanced dissipation rate due to planetary rotation. This model was thus able to reproduce the observed annual cyclic variation.

A fourth mechanism, mostly of importance over seasonal time scales, is penetrative convection. This mechanism has not been discussed in this report.

Differential (non-integral) models have been considered through a description of the model due to Mellor & Durbin *[19]*. These have the advantage of predicting the formation of a mixed layer rather than pre-supposing its existence and, in particular, they do not need to assume a vertically uniform velocity profile. Indeed the models due to Mellor & Durbin *[19]*, Marchek et al *[24]* and Warn-Varnas & Piacsek *[26]* all indicate the development and persistence of vertical shear throughout the entire mixed layer, provided that the wind does not abate appreciably. Since the principal justification for the integral or bulk model (apparently supported by observations) due to Gonella *[29]*, Pollard & Millard *[30]*, Pollard *[31]* and Pollard et al *[5]* is that the velocity has approximately no vertical shear through a large portion of the mixed layer, some mechanism to diminish the shear would appear to be missing from the differential models. This same mechanism way well not be accounted for properly in the integral models either.

This report does not make extensive comparison between models and observations but rather is intended to clarify theoretical differences between the various models themselves.

APPENDIX

APPENDIX A

The notations used, when not defined, are those of the Main Text. Tensor notation is used in some of the equations.

A.1 The mixed-layer momentum equation

The momentum balance can be expressed in the form

$$\frac{\partial u_i}{\partial t} + u_j \frac{\partial u_i}{\partial x_j} + \frac{\partial}{\partial x_i}\left(\frac{P}{\rho_o}\right) + \varepsilon_{ijk}\,\Omega_j\,U_k + \delta_{i3}\frac{g\rho}{\rho_o} - \nu \frac{\partial^2 u_i}{\partial x_j \partial x_j} = 0 \quad , \qquad \text{(Eq. A.1)}$$

where ε_{ijk} is the tensor operator ($\varepsilon_{ijk}\,\Omega_j\,u_k = \underline{\Omega} \times \underline{u}$), Ω_i is the earth's rotation vector, ρ is the pressure variable, and ν the molecular-diffusion coefficient. Setting $u_i = \bar{u}_i + u_i'$ and taking the average in time gives

$$\frac{\partial \bar{u}_i}{\partial t} + \overline{u_j' \frac{\partial u_i'}{\partial x_j}} + \bar{u}_j \frac{\partial \bar{u}_i}{\partial x_j} + \frac{\partial}{\partial x_i}\left(\frac{P}{\rho_o}\right) + \delta_{i3}\frac{g\bar{\rho}}{\rho_o} + \varepsilon_{ijk}\,\Omega_j\,\bar{u}_k - \nu \frac{\partial^2 \bar{u}_i}{\partial x_j\,\partial x_j} = 0 \quad . \qquad \text{(Eq. A.2)}$$

Applying the horizontal-homogeneity condition $\left(\frac{\partial}{\partial x_1} = \frac{\partial}{\partial x_2} = 0\right)$ and neglecting the molecular-diffusion term leaves, for the horizontal momentum balance,

$$\frac{\partial \underline{\bar{u}}}{\partial t} + \overline{w' \frac{\partial u'}{\partial z}} + \bar{w}\frac{\partial \underline{\bar{u}}}{\partial z} + \underline{f} \times \underline{\bar{u}} = 0 \quad . \qquad \text{(Eq. A.3)}$$

Next we set the upwelling velocity $\bar{w}$ to zero and apply the continuity condition

$$\frac{\partial u_j}{\partial x_j} = 0 \qquad \text{(Eq. A.4)}$$

to Eq. A.3 to give

$$\frac{\partial \underline{\bar{u}}}{\partial t} + \underline{f} \times \underline{\bar{u}} + \frac{\partial}{\partial z}(\overline{w'\underline{u}'}) = 0 \qquad \text{(Eq. A.5)}$$

and, after vertical integration from below the mixed layer,

$$\frac{\partial}{\partial t}\left(\int_{-H}^{0} \underline{\bar{u}}\, dz \right) + \underline{f} \times \left(\int_{-H}^{0} \underline{\bar{u}}\, dz \right) + (\overline{w'\underline{u}'})_0 - (\overline{w'\underline{u}'})_{-H} = 0. \qquad \text{(Eq. A.6)}$$

The last term on the left-hand side of Eq. A.6 vanishes if no motion is assumed at $Z = -H$. Equation A.6 then leads directly to the mixed-layer momentum equation (Eq. 9) of the Main Text.

A.2 The lower momentum flux-boundary condition

Term-by-term integration of Eq. A.5 across the lower interface, remembering that $\underline{u} = w = 0$ *for* $Z < -h-\delta$, *gives*

$$\int_{-h-\delta}^{-h} \frac{\partial \underline{\bar{u}}}{\partial t}\, dz = \frac{\partial}{\partial t}(\delta \underline{u} + o(\delta^2)) + \underline{\bar{u}}_h \frac{\partial h}{\partial t} ,$$

$$\int_{-h-\delta}^{-h} \underline{f} \times \underline{\bar{u}}\, dz = \delta(\underline{f} \times \underline{\bar{u}}_{-h}) + o(\delta^2) ,$$

$$\int_{-h-\delta}^{-h} \frac{\partial}{\partial z}(\overline{w'\underline{u}'})\, dz = (\overline{\underline{u}'w'})_{-h} .$$

Letting $\delta \to o$ leaves

$$(\overline{\underline{u}'w'})_{-h} = - \underline{\bar{u}}_{-h} \frac{\partial h}{\partial t} . \qquad \text{(Eq. A.7)}$$

Equation 11 of the Main Text is then obtained by assuming a slab-flow mixed layer.

A.3 The mean flow kinetic energy equation

Multiplying Eq. A.2 by $\bar{u}_i$, using the continuity condition of Eq. A.4, and neglecting molecular diffusion, leads to

$$\frac{\partial}{\partial t}\left(\frac{\bar{u}_i^2}{2}\right) + \frac{\partial}{\partial x_j}\left(\bar{u}_i\ \overline{u_j' u_i'}\right) - \overline{u_j' u_i'}\ \frac{\partial \bar{u}_i}{\partial x_j} + \bar{u}_j\ \frac{\partial}{\partial x_j}\left(\frac{\bar{u}_i^2}{2}\right)$$

$$+ \frac{g}{\rho_o}\,\bar{w}\,\bar{\rho} = 0 \quad .$$

Applying horizontal homogeneity and neglecting upwelling leaves

$$\frac{\partial}{\partial t}\left(\frac{\bar{\underline{u}} \cdot \bar{\underline{u}}}{2}\right) + \frac{\partial}{\partial z}\left(\bar{\underline{u}} \cdot \overline{\underline{u}'w'}\right) - \overline{\underline{u}'w'} \cdot \frac{\partial \bar{\underline{u}}}{\partial z} = 0 \quad . \qquad \text{(Eq. A.8)}$$

Vertical integration of Eq. A.8 from $Z = -H$ then yields Eq. 1 of the Main Text.

A.4 The turbulent kinetic energy balance

The turbulent momentum equation is obtained by subtracting Eq. A.2 from Eq. A.1 to give

$$\frac{\partial u_i'}{\partial t} + u_j' \frac{\partial u_i'}{\partial x_j} - \overline{\frac{\partial u_j'}{\partial x_j}} + u_j' \frac{\partial \bar{u}_i}{\partial x_j} + \bar{u}_j \frac{\partial u_i'}{\partial x_j}$$

$$+ \delta_{i3} \frac{g\rho'}{\rho_o} + \frac{\partial}{\partial x_i}\left(\frac{P'}{\rho_o}\right) - \nu \frac{\partial^2 u_i'}{\partial x_j \partial x_j} = 0 \quad . \qquad \text{(Eq. A.9)}$$

Multiplication of Eq. A.9 by u_i' and averaging yields

$$\frac{\partial}{\partial t}\left(\frac{\overline{u_i'^2}}{2}\right) + \frac{\partial}{\partial x_j} \overline{u_j' \frac{u_i'^2}{2}} + \delta_{ij}\ \overline{u_i' \frac{p'}{\rho_o}} + \overline{u_i' u_j'}\ \frac{\partial}{\partial x_j}\bar{u}_i$$

$$+ \frac{g}{\rho_o}\left(\overline{u_i' \rho'}\right) + \bar{u}_j \frac{\partial}{\partial x_j}\left(\frac{\overline{u_i'^2}}{2}\right) - \nu \frac{\partial^2}{\partial x_j \partial x_j}\left(\frac{\overline{u_i'^2}}{2}\right)$$

$$+ \nu \overline{\frac{\partial u'_i}{\partial x_j} \frac{\partial u'_i}{\partial x_j}} = 0 \qquad \text{(Eq. A.10)}$$

Applying horizontal homogeneity and neglecting upwelling leaves

$$\frac{\partial}{\partial t}\left(\frac{\overline{u_i'^2}}{2}\right) + \frac{\partial}{\partial z}\left[\overline{w'\frac{u_i'^2}{2}} + \overline{w'\frac{p'}{\rho_o}}\right] + \overline{\underline{u}'w'}\frac{\partial \bar{\underline{u}}}{\partial z}$$

$$+ \frac{g}{\rho_o}\left(\overline{u_i'\rho'}\right) - \nu\frac{\partial^2}{\partial x_j \partial x_j}\left(\frac{\overline{u_i^2}}{2}\right) + \varepsilon = 0 \quad , \qquad \text{(Eq. A.11)}$$

which, after vertical integration from $Z = -H$ and neglecting the upper and lower contributions from molecular diffusion leads to Eq. 2 of the Main Text.

A.5 The Reynolds shear stress contribution

Referring to Fig. A.1, the integrated Reynolds shear stress term can be written as

$$\int_{-H}^{o} \left(\overline{\underline{u}'w'}\right)\frac{\partial \bar{\underline{u}}}{\partial z}\,dz = \int_{-d}^{o} \left(\overline{\underline{u}'w'}\right)\frac{\partial \bar{\underline{u}}}{\partial z}\,dz + \int_{-h-\delta}^{-h} \left(\overline{\underline{u}'w'}\right)\frac{\partial \bar{\underline{u}}}{\partial z}\,dz \qquad \text{(Eq. A.12)}$$

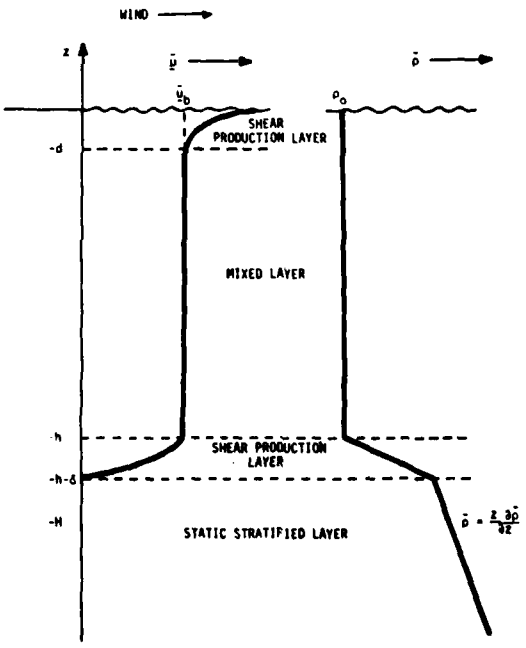

FIG. A.1

For the first term on the right-hand side of Eq. A.12 a constant-stress layer is usually assumed, so that

$$\int_{-d}^{o} \left(\overline{\underline{u}'w'}\right)\frac{\partial \bar{\underline{u}}}{\partial z}\,dz = \left(\overline{\underline{u}'w'}\right)_o \left(\bar{\underline{u}}_o - \bar{\underline{u}}_{-d}\right) \quad . \qquad \text{(Eq. A.13)}$$

For the second term on the right-hand side of Eq. A.12 we let $\delta \to o$ and approximate the stress in the interval $[-h, -h-\delta]$ by boundary condition Eq. A.7, so that

$$\int_{-h-\delta}^{-h} (\overline{\underline{u}'w'}) \frac{\partial \overline{\underline{u}}}{\partial z}\, dz \approx - \frac{\partial h}{\partial t} \int_{-h-\delta}^{-h} \overline{\underline{u}} \cdot \frac{\partial}{\partial z} \overline{\underline{u}}\, dz$$

$$= - \frac{\overline{\underline{u}} \cdot \overline{\underline{u}}}{2} \frac{\partial h}{\partial t} \quad . \qquad \text{(Eq. A.14)}$$

Expressions A.13 and A.14 combine to form the energy production term of Eq. 39 of the Main Text.

A.6 Potential energy for a deepening mixed layer

The changing potential energy of a deepening mixed layer can be expressed by

$$\frac{\partial \overline{PE}}{\partial t} = \lim_{\Delta t \to o} \frac{g}{\Delta t} \left\{ \int_{-\infty}^{o} \overline{\rho}(t+\Delta t) z\, dz - \int_{-\infty}^{o} \overline{\rho}(t) z\, dz \right\} . \qquad \text{(Eq. A.15)}$$

Next we consider the geometry of Fig. A.2.

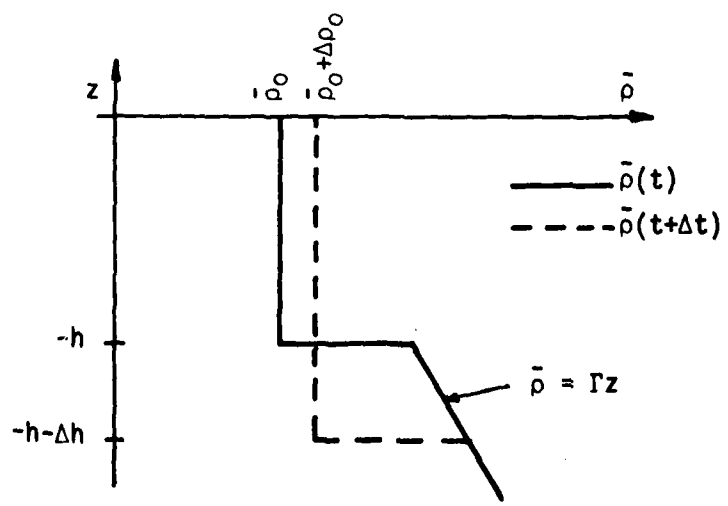

FIG. A.2

and express the difference between the braced integrals of Eq. A.15 in the interval [-h, o] as

$$\int_{-h}^{o} \Delta\rho_o \, z \, dz = \Delta\rho_o \frac{h^2}{2} \qquad \text{(Eq. A.16)}$$

and in the interval [-h-Δh, -h] as

$$\int_{-h-\Delta h}^{-h} ((\bar{\rho}_o + \Delta\bar{\rho}_o) - \Gamma z) \, z \, dz = - \bar{\rho}_o h\Delta h + \Gamma h^2 \Delta h + o(\Delta h^2, \Delta h \Delta\rho_o). \qquad \text{(Eq. A.17)}$$

Combining Eqs. A.16 and A.17 and substituting them into Eq. A.15 yields

$$\overline{\frac{\partial PE}{\partial t}} = - g \frac{h^2}{2} \frac{\partial\bar{\rho}_o}{\partial t} - gh(\bar{\rho}_o - \Gamma h) \frac{\partial h}{\partial t} + \int_{-\infty}^{-h} gz \frac{\partial\bar{\rho}}{\partial t} \, dz \quad . \qquad \text{(Eq. A.18)}$$

We then set $\Gamma h = \bar{\rho}_{-h-\delta}$ and note that Eq. A.18 is equivalent to Eq. 6 of the Main Text.

A.7 The lower mass flux-boundary condition

Term-by-term integration of the mass conservation equation of Eq. 4 of the Main Text across the lower interface gives

$$\int_{-h-\delta}^{-h} \frac{\partial\bar{\rho}}{\partial t} \, dz = \frac{\partial}{\partial t} (\delta\bar{\rho} + o(\delta^2)) + \bar{\rho}_{-h} \frac{\partial h}{\partial t} - \bar{\rho}_{-h-\delta} \frac{\partial h}{\partial t}$$

$$\int_{-h-\delta}^{-h} \frac{\partial}{\partial z} (\overline{w'\rho'} + \frac{\alpha}{c} I) \, dz = (\overline{w'\rho'})_{-h} + \frac{\alpha\delta}{c\gamma} I_o$$

letting $\delta \to o$ leaves

$$(\overline{w'\rho'})_{-h} = -(\bar{\rho}_{-h} - \bar{\rho}_{-h-\delta}) \frac{\partial h}{\partial t}$$

which is the boundary condition in Eq. 7 of the Main Text.

REFERENCES

1. NIILER, P.P. and KRAUS, E.B. ed. 1977: One-dimensional modèls of the upper ocean. In: Modelling and Prediction of the Upper Layers of the Ocean. Selected paper presented at a NATO sponsored Advance Study Institute held at Urbino, Italy. September, 1975. Oxford, U.K. , Pergamon Press, 1977: 143-172.

2. KIM, J.W. A generalized bulk model of the oceanic mixed layer. Journal of Physical Oceanography, 6, 1976: 686-695.

3. ZILITINKEVICH, S.S. CHALIKOV, D.V., RESNYANSKY, Yu D. and SHIRSHOV, P.P. Modelling the oceanic upper layer. Oceanologica Acta, 2, 1979: 219-240.

4. KRAUS, E.B. and TURNER J.S. A one-dimensional model of the seasonal thermocline: II. The general theory and its consequences. Tellus, 19, 1967: 98-106.

5. POLLARD, R.T., RHINES, P.B. and THOMPSON, R.O.R.Y. The deepening of the wind mixed layer. Geophysical Fluid Dynamics, 3, 1973, 381-404.

6. NIILER, P.P. Deepening of the wind-mixed layer. Journal of Marine Research, 33, 1975: 405-422.

7. GARWOOD, Jr. R.W. An oceanic mixed layer model capable of simulating cyclic states. Journal Physical Oceanography, 7, 1977: 455-468.

8. DENMAN, K.L. A time-dependent model of the upper ocean. Journal Physical Oceanography, 3, 1973: 173-184.

9. TURNER, J.S. and KRAUS, E.B. A one-dimensional model of the seasonal thermocline - I: A laboratory experiment and its interpretation. Tellus, 19, 1967: 88-97.

10. TABATA, S. and GIOVANDO, L.F. The seasonal thermocline at Ocean Weather Station 'P' during 1956 through 1959, Manuscript Report Series No. 157. Fisheries Research Board of Canada, 1963.

11. KATO, H. and PHILLIPS, O.M. On the penetration of a turbulent layer into stratified fluid. Journal of Fluid Mechanics , 37, 1969: 643-655.

12. MOORE, M.J. and LONG, R.R. An experimental investigation of turbulent stratified shearing flow. Journal of Fluid Mechanics, 49, 1971: 635-655.

13. TURNER, J.S. A note on-wind mixing at the seasonal thermocline, Deep Sea Research, 16, (Suppl.), 1969: 297-300.

14. DENMAN, K.L. and MIYAKE, M. Upper layer modification at ocean station PAPA: observations and simulation. Journal of Physical Oceanography, 3, 1973: 185-196.

15. MARTIN, P.J. and THOMPSON, J.D. Formulation and testing of a layer compatible upper ocean mixed-layer model, 1979: private communication.

16. TURNER, J.S. The influence of molecular diffusivity on turbulent entrainment across a density interface. Journal of Fluid Mechanics, 33, 1968: 639-656.

17. WYATT, L.R. Mixing and stratifying processes in the oceanic surface layer and seasonal thermocline, Ph. D. Thesis. University of Southampton, U.K., 1976.

18. KANTHA, L.H. Turbulent entrainment at the density interface of a two-layer stably stratified fluid system, TR 75-1. Baltimore, Md, Johns Hopkins University, Geophysical Fluid Dynamics Laboratory, 1975.

19. MELLOR, G.L. and DURBIN, P.A. The structure and dynamics of the ocean surface mixed layer, Journal of Physical Oceanography, 5, 1975: 718-728.

20. MUNK, W.H. and ANDERSON, E.R. Notes on a theory of the thermocline. Journal of Marine Research, 7, 1948: 276-295.

21. MELLOR, G.L. and YAMADA, T. A hierarchy of turbulence closure models for planetary boundary layers. Journal of the Atmospheric Sciences, 31, 1974: 1791-1806.

22. MINKLEY, B. Oceanographic observations at Ocean station P(50°N,145°W), Vol. 46, May 15 - July 1, 1970, Report 71-5. Ontario, Canada, Department of the Environment, Marine Sciences Branch, Pacific Region, 1971.

23. POLLARD, R.T. The Joint Air-Sea Interaction Trial, JASIN. Mémoires Société Royale des Sciences de Liège, 6, 1973: 17-34.

24. MARCHUK, G.I., KOCHERGIN, V.P., KLIMOK, V.I. and SUKHORUKOV, V.A., On the dynamics of the ocean surface mixed layer, Journal of Physical Oceanography, 7, 1977: 865-875.

25. HALPERN, D. Observations of the deepening of the wind-mixed layer in the Northeast Pacific Ocean, Journal of Physical Oceanography, 4, 1974: 454-466.

26. WARN-VARNAS, A.C. and PIACSEK, S.A. An investigation of the importance of third-order correlations and choice of length scale in mixed layer modelling. Geophysical and Astrophysical Fluid Dynamics, 13, 1979: 225-243.

27. ROTTA, J.C. Statistiche Theorie nichthomogener Turbulenz. Zeitschritt für Physik, 129, 1951: 547-572.

28. LUMLEY, J.L. and KHAJEH-NOURI, B. Computational modelling of turbulent transport, Advances in Geophysics, 18A, 1974: 169-192.

29. GONELLA, J. The drift current from observations made on the Bouee Laboratoire, Cahiers Océanographiques, 23, 1971: 1-15.

30. POLLARD, R.T. and MILLARD, R.C. Jr. Comparison between observed and simuated wind-generated inertial oscillations, Deep Sea Research, 17, 1970: 813-821.

31. POLLARD, R.T. Properties of near-surface inertial oscillations, Unpublished Manuscript, 1972.

INITIAL DISTRIBUTION

	Copies
MINISTRIES OF DEFENCE	
MOD Belgium	2
DND Canada	10
CHOD Denmark	8
MOD France	8
MOD Germany	15
MOD Greece	11
MOD Italy	10
MOD Netherlands	12
CHOD Norway	10
MOD Portugal	5
MOD Turkey	5
MOD U.K.	16
SECDEF U.S.	61
NATO AUTHORITIES	
Defence Planning Committee	3
NAMILCOM	2
SACLANT	10
SACLANTREPEUR	1
CINCWESTLANT/COMOCEANLANT	1
COMIBERLANT	1
CINCEASTLANT	1
COMSUBACLANT	1
COMMAIREASTLANT	1
SACEUR	2
CINCNORTH	1
CINCSOUTH	1
COMNAVSOUTH	1
COMSTRIKFORSOUTH	1
COMEDCENT	1
COMMARAIRMED	1
CINCHAN	1
SCNR FOR ARMAMENTS	
SCNR Belgium	1
SCNR Canada	1
SCNR Denmark	1
SCNR Germany	1
SCNR Greece	1
SCNR Italy	1
SCNR Netherlands	1
SCNR Norway	1
SCNR Portugal	1
SCNR Turkey	1
SCNR U.K.	1
SCNR U.S.	1
SECDEF Rep. SCNR	1
NAMILCOM Rep. SCNR	1
NATIONAL LIAISON OFFICERS	
NLO Canada	1
NLO Denmark	1
NLO Germany	1
NLO Italy	1
NLO U.K.	1
NLO U.S.	1
NLR TO SACLANT	
NLR Belgium	1
NLR Canada	1
NLR Denmark	1
NLR France	1
NLR Germany	1
NLR Greece	1
NLR Italy	1
NLR Netherlands	1
NLR Norway	1
NLR Portugal	1
NLR Turkey	1
NLR U.K.	1
NLR U.S.	1